cardiomyocyte apoptosis is unknown. Further investigation is required to understand the precise mechanisms of the antiapoptotic signaling pathway by ET-1 in the myocardium.

In summary, we demonstrated a novel signaling pathway for the antiapoptotic effect of ET-1 in cardiac myocytes. ET-1 prevents serum deprivation–induced apoptosis in cardiac myocytes via the ET_A receptor. c-Src is activated by ET-1, upregulates Bcl-x_L expression, and shows an antiapoptotic effect in cardiac myocytes. Collectively, these findings indicate a potentially important role for the c-Src/Bcl-x_L pathway in the antiapoptotic effect of ET-1. Because the loss of contractile cardiac myocytes due to apoptosis results in a further decrease of cardiac function, identification of the signaling pathway that mediates survival and/or apoptosis in cardiac myocytes is important. Thus, our data provide new insight into the molecular basis and therapeutic target for several cardiovascular diseases, including CHF and ischemic heart disease.

Acknowledgments

This study was supported by grants from the Ministry of Education, Science, Sports and Culture and the Kanae Foundation for Life and Socio-Medical Science. We thank Toshiko Kambe, Yuki Onuma, and Megumi Hata for their expert technical assistance.

References

1. Haunstetter A, Izumo S. Apoptosis: basic mechanisms and implications for cardiovascular disease. *Circ Res.* 1998;82:1111–1129.
2. MacLellan WR, Schneider MD. Death by design: programmed cell death in cardiovascular biology and disease. *Circ Res.* 1997;81:137–144.
3. Narula J, Haider N, Virmani R, DiSalvo TG, Kolodgie FD, Hajjar RJ, Schmidt U, Semigran MJ, Dec GW, Khaw BA. Apoptosis in myocytes in end-stage heart failure. *N Engl J Med.* 1996;335:1182–1189.
4. Kanoh M, Takemura G, Misao J, Hayakawa Y, Aoyama T, Nishigaki K, Noda T, Fujiwara T, Fukuda K, Minatoguchi S, Fujiwara H. Significance of myocytes with positive DNA in situ nick end-labeling (TUNEL) in hearts with dilated cardiomyopathy: not apoptosis but DNA repair. *Circulation.* 1999;99:2757–2764.
5. Mallat Z, Tedgui A, Fontaliran F, Frank R, Durigon M, Fontaine G. Evidence of apoptosis in arrhythmogenic right ventricular dysplasia. *N Engl J Med.* 1996;335:1190–1196.
6. Saraste A, Pulkki K, Kallajoki M, Henriksen K, Parvinen M, Voipio-Pulkki LM. Apoptosis in human acute myocardial infarction. *Circulation.* 1997;95:320–323.
7. Swynghedauw B. Molecular mechanisms of myocardial remodeling. *Physiol Rev.* 1999;79:215–262.
8. Buerke M, Murohara T, Skurk C, Nuss C, Tomaselli K, Lefer AM. Cardioprotective effect of insulin-like growth factor I in myocardial ischemia followed by reperfusion. *Proc Natl Acad Sci U S A.* 1995;92:8031–8035.
9. Fujio Y, Kunisada K, Hirota H, Yamauchi-Takihara K, Kishimoto T. Signals through gp130 upregulate bcl-x gene expression via STAT1-binding *cis*-element in cardiac myocytes. *J Clin Invest.* 1997;99:2898–2905.
10. Zhao YY, Sawyer DR, Baliga RR, Opel DJ, Han X, Marchionni MA, Kelly RA. Neuregulins promote survival and growth of cardiac myocytes: persistence of ErbB2 and ErbB4 expression in neonatal and adult ventricular myocytes. *J Biol Chem.* 1998;273:10261–10269.
11. Sheng Z, Knowlton K, Chen J, Hoshijima M, Brown JH, Chien KR. Cardiotrophin 1 (CT-1) inhibition of cardiac myocyte apoptosis via a mitogen-activated protein kinase-dependent pathway: divergence from downstream CT-1 signals for myocardial cell hypertrophy. *J Biol Chem.* 1997;272:5783–5791.
12. Rokosh DG, Stewart AF, Chang KC, Bailey BA, Karliner JS, Camacho SA, Long CS, Simpson PC. α1-Adrenergic receptor subtype mRNAs are differentially regulated by α1-adrenergic and other hypertrophic stimuli in cardiac myocytes in culture and in vivo: repression of α1B and α1D but induction of α1C. *J Biol Chem.* 1996;271:5839–5843.
13. Kajstura J, Cigola E, Malhotra A, Li P, Cheng W, Meggs LG, Anversa P. Angiotensin II induces apoptosis of adult ventricular myocytes in vitro. *J Mol Cell Cardiol.* 1997;29:859–870.
14. Singh K, Balligand JL, Fischer TA, Smith TW, Kelly RA. Regulation of cytokine-inducible nitric oxide synthase in cardiac myocytes and microvascular endothelial cells: role of extracellular signal-regulated kinases 1 and 2 (ERK1/ERK2) and STAT1α. *J Biol Chem.* 1996;271:1111–1117.
15. Shubeita HE, McDonough PM, Harris AN, Knowlton KU, Glembotski CC, Brown JH, Chien KR. Endothelin induction of inositol phospholipid hydrolysis, sarcomere assembly, and cardiac gene expression in ventricular myocytes: a paracrine mechanism for myocardial cell hypertrophy. *J Biol Chem.* 1990;265:20555–20562.
16. Bogoyevitch MA, Glennon PE, Andersson MB, Clerk A, Lazou A, Marshall CJ, Parker PJ, Sugden PH. Endothelin-1 and fibroblast growth factors stimulate the mitogen-activated protein kinase signaling cascade in cardiac myocytes: the potential role of the cascade in the integration of two signaling pathways leading to myocyte hypertrophy. *J Biol Chem.* 1994;269:1110–1119.
17. Spieker LE, Noll G, Ruschitzka FT, Luscher TF. Endothelin receptor antagonists in congestive heart failure: a new therapeutic principle for the future? *J Am Coll Cardiol.* 2001;37:1493–1505.
18. McMurray JJ, Ray SG, Abdullah I, Dargie HJ, Morton JJ. Plasma endothelin in chronic heart failure. *Circulation.* 1992;85:1374–1379.
19. Wei CM, Lerman A, Rodeheffer RJ, McGregor CG, Brandt RR, Wright S, Heublein DM, Kao PC, Edwards WD, Burnett JC Jr. Endothelin in human congestive heart failure. *Circulation.* 1994;89:1580–1586.
20. Miyauchi T, Yanagisawa M, Tomizawa T, Sugishita Y, Suzuki N, Fujino M, Ajisaka R, Goto K, Masaki T. Increased plasma concentrations of endothelin-1 and big endothelin-1 in acute myocardial infarction. *Lancet.* 1989;2:53–54.
21. Omland T, Lie RT, Aakvaag A, Aarsland T, Dickstein K. Plasma endothelin determination as a prognostic indicator of 1-year mortality after acute myocardial infarction. *Circulation.* 1994;89:1573–1579.
22. Shichiri M, Kato H, Marumo F, Hirata Y. Endothelin-1 as an autocrine/paracrine apoptosis survival factor for endothelial cells. *Hypertension.* 1997;30:1198–1203.
23. Cattaruzza M, Dimigen C, Ehrenreich H, Hecker M. Stretch-induced endothelin B receptor-mediated apoptosis in vascular smooth muscle cells. *FASEB J.* 2000;14:991–998.
24. Kakita T, Hasegawa K, Iwai-Kanai E, Adachi S, Morimoto T, Wada H, Kawamura T, Yanazume T, Sasayama S. Calcineurin pathway is required for endothelin-1–mediated protection against oxidant stress–induced apoptosis in cardiac myocytes. *Circ Res.* 2001;88:1239–1246.
25. Araki M, Hasegawa K, Iwai-Kanai E, Fujita M, Sawamura T, Kakita T, Wada H, Morimoto T, Sasayama S. Endothelin-1 as a protective factor against β-adrenergic agonist- induced apoptosis in cardiac myocytes. *J Am Coll Cardiol.* 2000;36:1411–1418.
26. Kamitani T, Ikeda U, Muto S, Kawakami K, Nagano K, Tsuruya Y, Oguchi A, Yamamoto K, Hara Y, Kojima T, Medford RM, Shimada K. Regulation of Na,K-ATPase gene expression by thyroid hormone in rat cardiocytes. *Circ Res.* 1992;71:1457–1464.
27. Yamashita Y, Watanabe S, Miyazato A, Ohya K, Ikeda U, Shimada K, Komatsu N, Hatake K, Miura Y, Ozawa K, Mano H. Tec and Jak2 kinases cooperate to mediate cytokine-driven activation of c-fos transcription. *Blood.* 1998;91:1496–1507.
28. Takaoka A, Tanaka N, Mitani Y, Miyazaki T, Fujii H, Sato M, Kovarik P, Decker T, Schlessinger J, Taniguchi T. Protein tyrosine kinase Pyk2 mediates the Jak-dependent activation of MAPK and Stat1 in IFN-γ, but not IFN-α, signaling. *EMBO J.* 1999;18:2480–2488.
29. Okuda M, Takahashi M, Suero J, Murry CE, Traub O, Kawakatsu H, Berk BC. Shear stress stimulation of p130(cas) tyrosine phosphorylation requires calcium-dependent c-Src activation. *J Biol Chem.* 1999;274:26803–26809.
30. Takahashi M, Okazaki H, Ogata Y, Takeuchi K, Ikeda U, Shimada K. Lysophosphatidylcholine induces apoptosis in human endothelial cells through a p38-mitogen-activated protein kinase-dependent mechanism. *Atherosclerosis.* 2002;161:387–394.
31. Takahashi M, Ogata Y, Okazaki H, Takeuchi K, Kobayashi E, Ikeda U, Shimada K. Fluvastatin enhances apoptosis in cytokine-stimulated vascular smooth muscle cells. *J Cardiovasc Pharmacol.* 2002;39:310–317.
32. Hatch GM, Lee D, Man RY, Kroeger EA, Choy PC. On the mechanism of the losartan-mediated inhibition of phosphatidylcholine biosynthesis in H9c2 cells. *Biochim Biophys Acta.* 1997;1347:183–190.
33. Russell FD, Molenaar P. The human heart endothelin system: ET-1 synthesis, storage, release and effect. *Trends Pharmacol Sci.* 2000;21:353–359.

34. Haunstetter A, Izumo S. Future perspectives and potential implications of cardiac myocyte apoptosis. *Cardiovasc Res.* 2000;45:795–801.
35. Rosen K, Coll ML, Li A, Filmus J. Transforming growth factor-α prevents detachment-induced inhibition of c-Src kinase activity, Bcl-XL down-regulation, and apoptosis of intestinal epithelial cells. *J Biol Chem.* 2001;276: 37273–37279.
36. Jost M, Huggett TM, Kari C, Boise LH, Rodeck U. Epidermal growth factor receptor-dependent control of keratinocyte survival and Bcl-xL expression through a MEK-dependent pathway. *J Biol Chem.* 2001;276:6320–6326.
37. Karni R, Jove R, Levitzki A. Inhibition of pp60c-Src reduces Bcl-XL expression and reverses the transformed phenotype of cells overexpressing EGF and HER-2 receptors. *Oncogene.* 1999;18:4654–4662.
38. Yamauchi-Takihara K, Kishimoto T. A novel role for STAT3 in cardiac remodeling. *Trends Cardiovasc Med.* 2000;10:298–303.
39. Kang PM, Izumo S. Apoptosis and heart failure: a critical review of the literature. *Circ Res.* 2000;86:1107–113.
40. Arai H, Hori S, Aramori I, Ohkubo H, Nakanishi S. Cloning and expression of a cDNA encoding an endothelin receptor. *Nature.* 1990;348:730–732.
41. Sakurai T, Yanagisawa M, Takuwa Y, Miyazaki H, Kimura S, Goto K, Masaki T. Cloning of a cDNA encoding a non-isopeptide-selective subtype of the endothelin receptor. *Nature.* 1990;348:732–735.
42. Nakamura T, Mizuno S, Matsumoto K, Sawa Y, Matsuda H. Myocardial protection from ischemia/reperfusion injury by endogenous and exogenous HGF. *J Clin Invest.* 2000;106:1511–1519.
43. Abram CL, Courtneidge SA. Src family tyrosine kinases and growth factor signaling. *Exp Cell Res.* 2000;254:1–13.
44. Singh K, Communal C, Sawyer DB, Colucci WS. Adrenergic regulation of myocardial apoptosis. *Cardiovasc Res.* 2000;45:713–719.
45. Negoro S, Kunisada K, Tone E, Funamoto M, Oh H, Kishimoto T, Yamauchi-Takihara K. Activation of JAK/STAT pathway transduces cytoprotective signal in rat acute myocardial infarction. *Cardiovasc Res.* 2000;47:797–805.

Bruton's Tyrosine Kinase Is Required For Lipopolysaccharide-induced Tumor Necrosis Factor α Production

Nicole J. Horwood,[1] Tara Mahon,[1] John P. McDaid,[1] Jamie Campbell,[1] Hiroyuki Mano,[2] Fionula M. Brennan,[1] David Webster,[3] and Brian M.J. Foxwell[1]

[1]*Kennedy Institute of Rheumatology Division, Faculty of Medicine, Imperial College of Science, Technology and Medicine, London W6 8LH, United Kingdom*
[2]*Jichi Medical School, Division of Functional Genomics, Tochigi 329-0498, Japan*
[3]*Royal Free Medical School, Department of Immunology, University College London, London NW3 2QG, United Kingdom*

Abstract

Lipopolysaccharide (LPS), a product of Gram-negative bacteria, is potent mediator of tumor necrosis factor (TNF)α production by myeloid/macrophage cells. Inhibitors capable of blocking the signaling events that result in TNFα production could provide useful therapeutics for treating septic shock and other inflammatory diseases. Broad spectrum tyrosine inhibitors are known to inhibit TNFα production, however, no particular family of tyrosine kinases has been shown to be essential for this process. Here we show that the Bruton's tyrosine kinase (Btk)-deficient mononuclear cells from X-linked agammaglobulinemia patients have impaired LPS-induced TNFα production and that LPS rapidly induces Btk kinase activity in normal monocytes. In addition, adenoviral overexpression of Btk in normal human monocytes enhanced TNFα production. We examined the role of Btk in TNFα production using luciferase reporter adenoviral constructs and have established that overexpression of Btk results in the stabilization of TNFα mRNA via the 3′ untranslated region. Stimulation with LPS also induced the activation of related tyrosine kinase, Tec, suggesting that the Tec family kinases are important components for LPS-induced TNFα production. This study provides the first clear evidence that tyrosine kinases of the Tec family, in particular Btk, are key elements of LPS-induced TNFα production and consequently may provide valuable therapeutic targets for intervention in inflammatory conditions.

Key words: tyrosine kinase • adenovirus • TNFα • macrophage • X-linked agammaglobulinemia

Introduction

TNFα is a proinflammatory cytokine pivotal to the pathogenesis of chronic inflammatory diseases such as rheumatoid arthritis and Crohn's disease (1), and in inflammatory responses such as leukocyte migration, tissue resorption, the acute-phase response, and fever (2). The major producers of TNFα are cells of the mononuclear phagocyte lineage including macrophages, microglia, osteoclasts, and myeloid dendritic cells. Despite considerable efforts, relatively few signaling molecules, e.g., nuclear factor (NF)*-κB (3, 4) and p38 MAPK/MK2 (5, 6), have been shown to be essential for TNFα expression in macrophages. It is well documented that tyrosine kinase inhibitors are potent suppressors of LPS-induced TNFα production (7, 8) and that

N.J. Horwood, T. Mahon, and J.P. McDaid contributed equally to this work.

Address correspondence to Brian M.J. Foxwell, Kennedy Institute of Rheumatology Division, Faculty of Medicine, Imperial College of Science, Technology and Medicine, Charing Cross Campus, ARC Building, 1 Aspenlea Road, London W6 8LH, United Kingdom. Phone: 44-208-383-4444; Fax: 44-208-383-4499; E-mail: b.foxwell@ic.ac.uk

*Abbreviations used in this paper: AdBtk, adenovirus-encoding human Bruton's tyrosine kinase; ARE, AU-rich element; Btk, Bruton's tyrosine kinase; IκBα, inhibitory protein κBα; MAPK, mitogen-activated protein kinase; m.o.i., multiplicity of infection; NF, nuclear factor; UTR, untranslated region; *xid*, X-linked immunodeficiency; XLA, X-linked agammaglobulinemia.

 J. Exp. Med. © The Rockefeller University Press • 0022-1007/2003/06/1603/9 $8.00
Volume 197, Number 12, June 16, 2003 1603–1611
http://www.jem.org/cgi/doi/10.1084/jem.20021845

the activation of tyrosine kinase activity is one of the earliest detectable events after LPS stimulation of monocytic cells (9–11). However, defining a causal relationship between a particular tyrosine kinase and TNFα production has been difficult. LPS can activate the Src family kinases $p58^{hck}$, $p53^{lyn}$, and $p59^{fgr}$, as well as $p72^{syk}$ (12–14), yet macrophages from mice deficient in these kinases do not show any impairment of LPS-induced TNFα production (15, 16). LPS has also been shown to activate the tyrosine kinase Pyk-2 (17), but its role, if any, in TNFα production has yet to be elucidated.

Another family of nonreceptor tyrosine kinases expressed by monocytic cells is the Tec family, and in particular, Bruton's tyrosine kinase (Btk). Recent studies have shown that the Tec family kinases are important components of both antigen receptor signaling and other cell surface receptors, resulting in the activation of numerous signal transduction pathways, regulation of the actin cytoskeleton, adhesion, migration, and transcriptional activation (18). Btk is found in all cells of the hematopoietic lineage except plasma and T cells (19), and is required for normal B cell development and signal transduction through cell surface molecules (20). Mutations in the *btk* gene result in aberrant B cell development, leading to the X-linked agammaglobulinemia (XLA) phenotype in humans and to the less severe X-linked immunodeficiency (*xid*) in mice. *xid* B cells show some hyporesponsiveness to LPS stimulation, although the precise cause has not been established (21, 22). Because the major phenotype of Btk deficiency is impaired B cell development and function, this cell type has been the major focus of interest to date. Earlier studies performed on *xid* mononuclear cells showed no obvious impairment of TNFα production in response to a series of inflammatory stimuli such as LPS and formalin-killed *Staphylococcus aureus* (23). However, bone marrow–derived cultured mast cells from *xid* mice have been shown to produce less TNFα in passive cutaneous anaphylactic reactions (24) and there is a recent report that *xid* peritoneal macrophages express reduced levels of TNFα and IL-1β in response to LPS (25). Additionally, *xid* mice are resistant to models of autoimmune diseases, e.g., collagen-induced arthritis (26, 27).

In humans, XLA is characterized by the absence of mature B cells in the periphery with a marked reduction in serum levels of all Ig isotypes resulting in a susceptibility to recurrent and severe bacterial infections (20, 28). Yet despite lacking Btk, XLA monocytes appear to develop normally and are present in expected numbers in the circulation. The importance of Btk in human monocyte/macrophages remains to be fully elucidated. As the XLA phenotype differs from that of the *xid* mice, we have examined the responses of XLA monocytes and macrophages to LPS stimulation. In addition, we have used an adenovirus expressing Btk in conjunction with TNFα luciferase reporter adenoviruses to analyze the contribution of Btk-dependent signaling events to the regulation of TNFα production.

Materials and Methods

Isolation and Culture of Cells

Isolation and Culture of PBMCs from XLA and Control Donors. Human blood samples were collected into lithium heparin vacutainers. Each blood sample was mixed with an equal volume of HBSS. PBMCs were prepared by ficoll-hypaque centrifugation on a lymphoprep gradient. PBMCs were cultured in RPMI containing 100 units/ml penicillin/streptomycin and 10% heat-inactivated FCS at 37°C in a humidified atmosphere containing 5% CO_2. Monocytes were isolated from the PBMCs by adherence to plastic for 1 h at 37°C in RPMI containing 100 units/ml penicillin/streptomycin and 10% FCS. Nonadherent cells were then washed off and the adherent monocytes were rested overnight and stimulated with LPS. B cells were depleted from PBMC using Dynabeads® coated with anti-CD19 antibodies. Cells were incubated with the beads for 1 h with constant agitation at 4°C. The beads were then magnetically removed and the remaining cells were subjected to FACS® analysis with FITC-conjugated anti-CD19 resulting in >90% B cell depletion.

Isolation of Monocytes by Elutriation. PBMCs were prepared from buffy coat fractions of a unit of blood from a single donor using ficoll-hypaque. The monocytes were then isolated by centrifugal elutriation as previously described (4). Monocyte fractions of >85% purity were routinely collected in this manner. Monocytes were cultured in RPMI containing 100 units/ml penicillin/streptomycin and 10% heat-inactivated FCS at 37°C in a humidified atmosphere containing 5% CO_2. For adenoviral infection, monocytes were treated with 100 ng/ml M-CSF (provided by G. Larsen, Genetics Institute, Boston, MA) for 72 h before viral infection.

Generation of Adenoviral Vectors and Cell Infection. Recombinant, replication-deficient adenoviral constructs encoding wild-type human Btk (AdBtk; cDNA provided by C. Kinnon, Institute of Child Health, London, United Kingdom) were prepared using the AdEasy system as previously described (29). In short, recombinant viral DNA was transfected into 293 cells in 6-well tissue culture plates using lipofectamine (GIBCO BRL) according to the manufacturer's instructions. Cells were overlaid with 2% agarose/DMEM 24 h after transfection and viral plaques were picked after 9–10 d. Viral clones were propagated in 293 cells and screened for transgene expression by Western blotting. Clonal viruses were then prepared from 20 175 cm^3 tissue culture flasks of 293 cells by ultracentrifugation through two caesium chloride gradients. Titres of viral stocks were determined by plaque assay and viral aliquots were stored at −70°C. The AdGFP adenovirus was prepared according to this protocol using AdTrackGFP with no insert. AdTrack0 (Ad0), pAdTrack-TNF 5′ promoter-Luc-3′ untranslated region (UTR; Ad5′3′luc), and pAdTrack-TNF 5′ promoter-Luc (Ad5′luc) were generated as previously described (30). The NF-κB luciferase adenovirus (AdNF-κB-luc) contains four tandem copies of the κ enhancer element located upstream of the firefly luciferase gene (31). This adenovirus was provided by P.B. McCray Jr. (University of Iowa, Iowa City, IA) and is a modification of the pNF-κB reporter vector (BD Clontech). Recombinant adenoviral vectors encoding *Escherichia coli* β-galactosidase (Adβgal) were provided by M. Woods and A. Bryne (Oxford University, Oxford, United Kingdom).

M-CSF–derived monocytes were plated in 96-well plates at 1.5×10^5 cells/well and allowed to settle for at least 4 h. The cells were washed in serum-free RPMI medium and then exposed to virus at different multiplicity of infection (m.o.i.) for 2 h

in serum-free RPMI at 37°C, after which cells were washed in RPMI and cultured in complete medium for 24 h before stimulation with LPS as previously described (4).

Immunoprecipitation and In Vitro Kinase Assay. Btk autokinase activity was measured in response to LPS in primary human monocytes. Cells were stimulated with LPS for various times as detailed. Cells were pelleted by centrifugation and lysed for 20 min on ice with 1% NP-40 lysis buffer containing 20 mM Tris, pH 8, 130 mM NaCl, 10 mM NaF, 1 mM DTT, 20 μM leupeptin, 100 μM sodium orthovanadate, 1 mM PMSF, 10 μM E64, and 2 mg/ml aprotinin. Lysates were microfuged for 10 min at 13,000 rpm at 4°C and supernatants were removed and precleared for 30 min at 4°C in 20 μl protein A–sepharose (previously washed in lysis buffer). After centrifuging the samples for 10 min at 1,300 rpm, the supernatants were removed and incubated with 2 μl rabbit polyclonal anti–Btk (provided C. Kinnon, Institute of Child Health, London, United Kingdom) for 1 h at 4°C. 30 μl protein A–sepharose was then added to each sample and incubated for an additional 1.5 h at 4°C. The beads were then washed three times in lysis buffer and once in kinase buffer (10 mM $MgCl_2$; 10 mM $MnCl_2$). Beads were mixed with kinase buffer containing γ^{32}P[ATP] and incubated for 15 min at room temperature. The reaction was stopped by the addition of 4× Laemmli buffer and the samples were boiled for 10 min. Samples were electrophoresed on an 8% SDS polyacrylamide gel. The gel was stained, fixed, dried, and autoradiographed. Tec autokinase activity was measured as previously described (32). Tec protein was immunoprecipitated, either with rabbit anti–Tec serum (32) or goat polyclonal anti–Tec (Santa Cruz Biotechnology, Inc.).

Western Blot Analysis. Cells were lysed in lysis buffer and debris pelleted as described above. Lysate protein concentration was assessed by Bradford assay and equivalent amounts of lysate protein were electrophoresed on 8% SDS polyacrylamide gels, followed by electrotransfer of proteins onto nitrocellulose membranes. Membranes were blocked in 10% Marvel/PBS/Tween (0.05%) and probed with either rabbit polyclonal anti–Btk (BD Biosciences) at 1 μg/ml in 5% Marvel/PBS/Tween (0.05%), anti–inhibitory protein κBα (IκBα; Santa Cruz Biotechnology, Inc.), anti-p54/JNK (Santa Cruz Biotechnology, Inc.), or rabbit anti–Tec for 2 h. After washing, membranes were incubated with anti–rabbit horseradish peroxidase at 1:5,000 in 5% Marvel/PBS/Tween (0.05%). After washing in PBS/Tween (0.05%), the membranes were developed using enhanced chemiluminescence according to the manufacturer's instructions (Amersham Biosciences).

ELISA. Supernatants were harvested 18 h after stimulation of human macrophages or PBMCs. The concentration of TNFα (BD Biosciences) was determined by ELISA according to the manufacturer's instruction. Absorbance was read and analyzed at 450 nM on a spectrophotometric ELISA plate reader (Labsystems Multiskan Biochromic) using the Ascent 2.4.2 software program. Results are expressed as the mean concentration of triplicate cultures ±SD.

Luciferase Assays. After LPS stimulation, cells were washed once in PBS and lysed with 100 μl CAT lysis buffer (0.65% [vol/vol] of NP-40, 10 mM Tris-HCl, pH 8, 0.1 mM EDTA, pH 8, 150 mM NaCl). 50 μl cell lysate were transferred into the well of a luminometer cuvette strip containing 120 μl luciferase assay buffer. Luciferase activity was measured with a Labsystem Luminometer by dispensing 30 μl luciferin (Bright-Glo luciferase assay system; Promega) per assay point. Cell lysates were assayed for protein concentration by Bradford assay and luciferase activity was adjusted accordingly.

Taqman RT-PCR. M-CSF–treated monocytes were plated at 5×10^5 cells/well in 24-well plates and infected as described above. Total RNA was extracted using RNeasy Kit (QIAGEN) according to the manufacturer's instructions. All semiquantitative RT-PCR was performed using an ABI PRISM 7700 Sequence Detection System, Taqman One Step RT-PCR reagent, and TNFα, IL-6, and GAPDH predeveloped assay reagents (Perkin-Elmer). ABI PRISM 7700 Sequence detector was programmed for the RT step of 30 min at 48°C followed by a 5-min deactivation step at 95°C. Subsequent PCR amplification consisted of 40 cycles of denaturation at 94°C for 15 s and annealing/extension at 60°C for 60 s. The cycle number at which the amplification plot crosses a fixed threshold above baseline is defined as threshold cycle (C_t). To control variation in mRNA concentration, all results were normalized to the housekeeping gene, GAPDH. Relative quantitation was performed using the comparative $\Delta\Delta C_t$ method according to the manufacturer's instructions.

Results

Btk Deficiency Results in Impaired TNFα Production. PBMCs from XLA blood were used to see if Btk deficiency had any effect on LPS-induced TNFα production. When compared with PBMC from normal age and sex-matched controls, the LPS response of XLA cells was impaired. At the lowest dose of LPS (0.1 ng/ml), XLA and normal PBMCs produced similar levels of TNFα, but increasing concentrations of LPS failed to generate the increased response seen in the normal cells. At 10 ng/ml, LPS-induced TNFα production by XLA PBMCs was only 15% of the control cells, whereas at 100 ng/ml LPS the response was only 10% of control (Fig. 1 A). Although B cells are not known to produce TNFα in response to LPS, the involvement of B cells from the normal PBMCs in LPS-induced TNFα production was investigated to negate any secondary effects due to the absence of B cells in XLA PBMCs. Depleting B cells from normal PBMC showed no effect on LPS-induced TNFα production (Fig. 1 B). Furthermore, we found that the T cells, the major component of PBMCs, did not produce TNFα in response to LPS (unpublished data) and these cells do not express Btk (33). Although the amount of blood available made purifying the monocytes from XLA blood difficult, we managed to separate the monocytic cells using adherence. LPS-induced TNFα production was again significantly reduced, although at 50% of normal controls, the impairment was not as great as seen in PBMCs (Fig. 1 C).

Stimulation with LPS Induces Btk Kinase Activity In Vitro. To further establish a role for Btk in LPS-induced TNFα production, we attempted to determine whether LPS was able to regulate Btk activity. Autokinase assays of enzyme immunoprecipitated from human primary monocytes demonstrated that LPS could rapidly activate Btk (Fig. 2 A). Btk autokinase activity was also observed in the murine macrophage cell line RAW 264.7 after LPS stimulation (unpublished data). Additionally, the effect of overexpression of Btk was examined by infecting 48-h M-CSF–treated monocytes (4) with increasing amounts of adenovirus-encoding human Btk (AdBtk). Infection with AdBtk

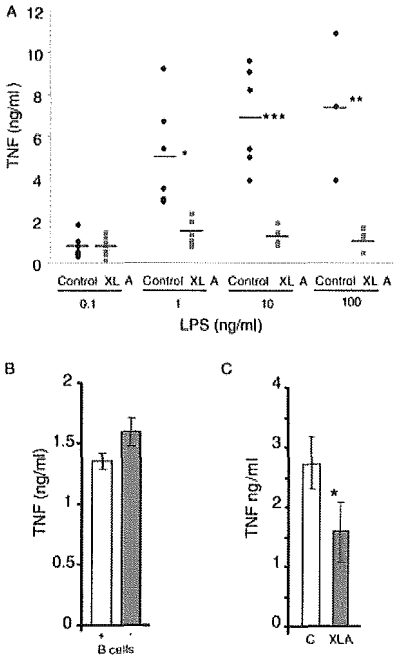

Figure 1. LPS-induced TNFα expression in PBMCs/monocytes from XLA and normal donors. (A) PBMCs from XLA and normal male donors (age range 17–38 yr). (B) Total PBMCs and PBMCs depleted of B cells from normal donors. (C) Monocytes prepared by adherence from normal and XLA PBMCs. Cells were stimulated with 10 ng/ml LPS (unless otherwise stated) for 18 h and supernatants were assayed for TNFα production by ELISA. In A, each point represents a donor, B is representative of three separate experiments, and C shows the combined results of five donors of each type (error bars ± SD). Results from Student's *t* test P values: *, $P < 0.05$; **, $P < 0.01$; ***, $P < 0.001$. TNFα production from unactivated cells was undetectable.

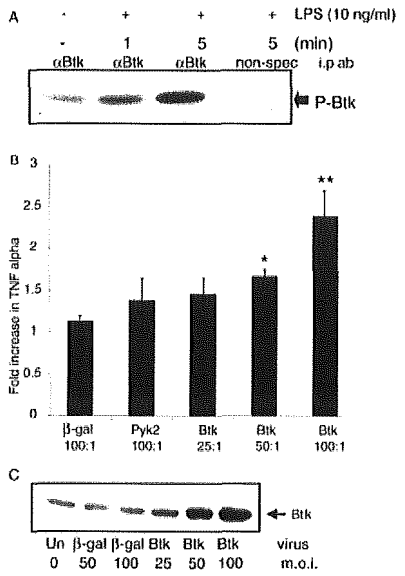

Figure 2. Btk is activated by LPS stimulation and modulates TNFα production. (A) Primary monocytes were stimulated with LPS for the indicated intervals. Cell lysates were immunoprecipitated and immune complex kinase assays were performed. Autophosphorylated Btk proteins were detected by autoradiography. This result is representative of three separate experiments. (B) Monocytes were infected with adenoviruses encoding either wild-type Btk (Btk WT), *β-galactosidase* (β-Gal), or an unrelated tyrosine kinase, Pyk2. Cells were stimulated with LPS for 18 h and the supernatants were assayed for TNFα expression. Data is presented as fold activation compared with uninfected LPS stimulated control cells (±SD). *, $P < 0.05$; **, $P < 0.01$ compared with LPS-activated uninfected controls. (C) Cell lysates from the infected cells were examined for Btk expression by immuno-Western blotting. Data is representative of at least four different donors.

alone did not induce TNFα production (unpublished data). However, infection with increasing amounts of virus synergized with LPS to increase TNFα expression, resulting in a two- to threefold increase in TNFα at the highest m.o.i. of 100 (Fig. 2 B). This effect correlated with the increased amounts of Btk protein seen in the infected cells (Fig. 2 C). No effect on TNFα production was seen with control viruses encoding either β-galactosidase or Pyk2, another LPS-activated tyrosine kinase (17), at the highest m.o.i. of 100 (Fig. 2 B).

LPS-induced IκBα Degradation Is Intact in XLA PBMCs. Overall, the data strongly suggested that there was a role for Btk in LPS-induced TNFα production. However, there was the possibility that this was the result of some development defect, rather than a direct effect of an absent kinase. As others have reported (34), FACS® analysis showed no impairment of CD14 expression, a component of the LPS binding on XLA monocytes (unpublished data). We also used the LPS-induced degradation of IκBα as a measure of signaling function, as this event does not appear to require tyrosine kinase activity (35, 36) and therefore should be intact. As shown in Fig. 3 A, there was a similar degradation of IκBα in XLA and normal monocytes in response to LPS, indicating no obvious impairment of the NF-κB activation pathway. We further investigated the involvement of the NF-κB signaling pathway by coinfecting M-CSF–treated monocytes with AdBtk and an NF-κB reporter virus that encodes luciferase under the control of a series of NF-κB binding sites (31). M-CSF monocytes were simultaneously infected with these viruses and controls, and the luciferase activity and TNFα production were measured after 18 h of LPS stimulation. Although we still observed an increase in TNFα production in these cultures (Fig. 3 C), there was no corresponding increase in luciferase activity (Fig. 3 B), indicating that Btk was able to promote TNFα production independently of the NF-κB activation.

Overexpression of Btk Acts via the 3′ UTR of TNF mRNA. To establish the mechanism of Btk action on TNFα production, the activity of the human TNF promoter in stimulated human macrophages was studied using 5′ promoter-luciferase and 5′ promoter-luciferase-3′ UTR adenoviral TNF gene reporter constructs (30). Primary human macrophages were simultaneously infected with reporter viruses at an m.o.i. of 40, whereas the Ad0 or AdBtk were used at an m.o.i. of 100. 24 h after adenoviral infection, macrophages were treated with LPS or left unstimulated for 18 h before assay of luciferase activity and ELISA for TNFα pro-

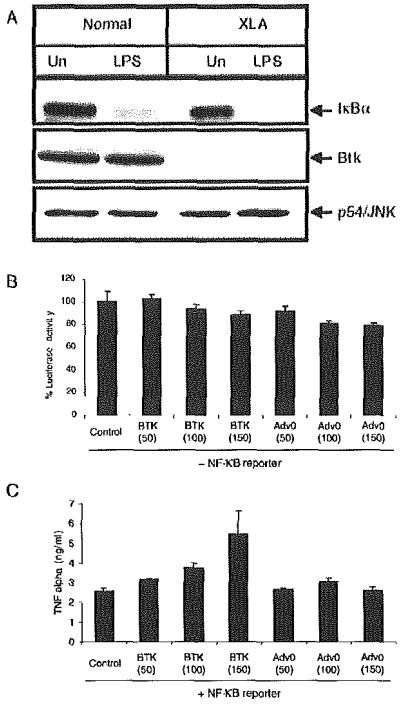

Figure 3. LPS-induced IκBα degradation in XLA and normal PBMCs. (A) PBMCs stimulated with 10 ng/ml LPS for 20 min were lysed and sequentially immunoblotted for the indicated proteins. This result is representative of three different experiments. (B and C) M-CSF monocytes were simultaneously infected with NF-κB luciferase reporter construct (m.o.i. of 100) alone, or coinfected with either AdBtk or Ad0 at various m.o.i. 24 h after adenoviral infection, cells were treated with LPS for 18 h before assay of (B) luciferase activity and (C) TNFα production. Data are means of triplicate cultures ± SD and are expressed as a percentage of the control level. This graph is representative of five experiments performed using different donors.

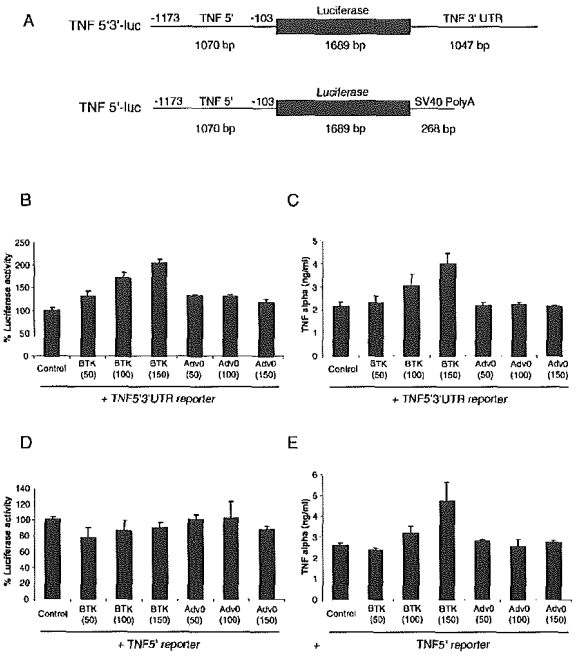

Figure 4. Btk overexpression enhances TNFα via the 3′ UTR. (A) Schematic representation of the human TNF 5′ promoter-luciferase-3′ UTR and TNF 5′ promoter-luciferase adenoviral constructs. Activity of the human TNF 5′ 3′ UTR (B and C) or TNF 5′ promoter (D and E) in stimulated human macrophages was tested by simultaneously infecting primary human macrophages with reporter virus at an m.o.i. of 40 and either Ad0 or AdBtk at various m.o.i. 24 h after adenoviral infection, macrophages were treated with LPS for 18 h before assay of luciferase activity (B and D) and TNFα production (C and E). Data are means of triplicate cultures ± SD and are expressed as a percentage of the control level. Each graph is representative of five experiments performed using different donors.

duction. There was a threefold increase in luciferase activity in the cells containing the TNF5′ 3′ UTR reporter construct compared with the Ad0 control cells (Fig. 4 A). However, there was no enhancement of luciferase activity from the TNF 5′ promoter construct (Fig. 4 C). Overexpression of Btk enhanced LPS-stimulated TNFα production by threefold in the presence of either TNF reporter construct (Fig. 4, B and D). There was no significant difference in TNF production and luciferase activity when comparing Ad0-infected macrophages with controls infected with the reporter constructs alone. The lack of enhanced luciferase activity from the 5′ promoter construct after LPS stimulation indicated that the 3′ UTR of TNFα mRNA was required for the action of Btk.

Overexpression of Btk Leads to Stabilization of TNFα mRNA. The importance of the 3′ UTR in the stability of TNFα mRNA has been studied extensively (37, 38). Because Btk appeared to be acting via the 3′ UTR, it seemed likely that it was also affecting the stability of TNFα mRNA. To further analyze the mechanism by which Btk determines the levels of TNFα, we blocked transcription in LPS-stimulated M-CSF monocytes by using actinomycin D and analyzed half-life of TNFα mRNA by Taqman RT-PCR analysis. As a control, GAPDH mRNA was detected and used to normalize the TNFα mRNA levels. For each of the controls, uninfected Ad0 and PykM, the half-life of TNFα mRNA was <45 min after actinomycin D treatment. However, in the presence of Btk, TNFα mRNA levels were maintained at 70–100% of the time 0 control for the duration of the 120-min time course (Fig. 5 A). These data demonstrate the ability of Btk to stabilize TNFα mRNA and consequently this may result in the elevated protein expression observed in these cultures.

As the stability of TNF mRNA is known to be associated with p38 mitogen-activated protein kinase (MAPK) activation, we examined the ability of PBMCs from XLA patients to phosphorylate p38 MAPK in response to LPS treatment. We were able to observe consistently low levels of p38 MAPK phosphorylation in XLA PBMCs (Fig. 5 B), however there was considerable variability in the degree of p38 MAPK phosphorylation from person to person in the normal controls. There was no difference in p38 MAPK phosphorylation after LPS treatment of normal PBMCs in either the presence or absence of B cells (unpublished data). Due to the limitation of patient samples we were unable to

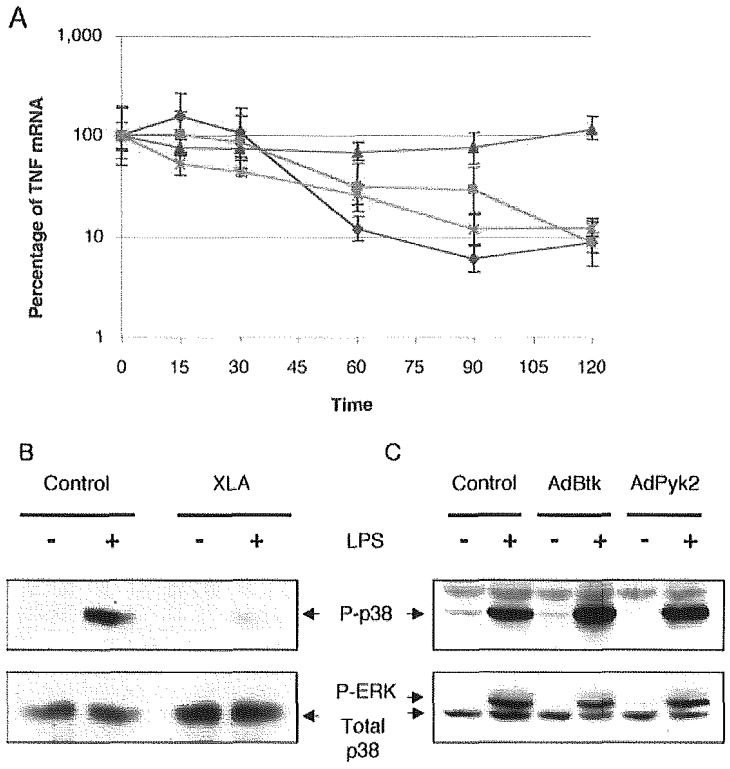

Figure 5. Btk overexpression stabilizes TNFα mRNA. (A) Cells were either uninfected or infected with Ad0, Ad PykM, or AdBtk (m.o.i. of 100) and activated with LPS for 4 h. 5 μg/ml actinomycin D was added to stop any further mRNA synthesis and the cells were incubated for an additional 0, 15, 30, 60, 90, or 120 min, after which time they were harvested in RNA lysis buffer and the supernatants were reserved for TNFα ELISA. Total mRNA was prepared and Taqman RT-PCR was used to access the quantity of TNFα. The results were normalized to 100% at the 0-min time point. The lines are representative of Control (◆), Ad0 (■), Btk (▲), and PykM (x). Data are means of triplicate reactions ± SD expressed as a percentage of the control and are representative of three experiments performed using different donors. (B) PBMCs from XLA and normal male donors or (C) M-CSF monocytes infected with AdBtk or AdPyk2, were stimulated with LPS for 20 min, lysed, and sequentially immunoblotted for the indicated proteins. These results are representative of three different experiments.

examine the kinetics of p38 MAPK activation in XLA patients compared with normal controls. To further establish the link between p38 MAPK and Btk, we used adenoviral overexpression of Btk to determine if there was any increase in p38 MAPK activity in normal M-CSF–treated monocytes. As shown in Fig. 5 C, we were able to observe a 1.5–2-fold increase in phosphorylated p38 MAPK.

Tec Is Phosphorylated in Response to LPS. Although we have demonstrated that Btk is able to modulate TNFα expression, XLA patients do not show a serious impairment in their innate immune function. Treatment of XLA monocytes for 2 d with M-CSF greatly enhanced their production of TNFα in response to LPS to levels similar to those obtained with normal monocytes (Fig. 6 A). Consequently, we examined the mechanism of the increased responsiveness of monocytes after M-CSF treatment. Because members of the Tec family of kinases can functionally complement each other (39), we tested whether M-CSF can regulate the expression of an alternative Tec family kinase to Btk. An obvious candidate was Tec kinase, as this enzyme is expressed in myeloid cells and does, to some degree, complement Btk activity in *xid* B cells (40). Western immunoblot analysis showed that Tec kinase was expressed at low levels in untreated monocytes from both normal donors and XLA patients (Fig. 6 B), however, after treatment with M-CSF for 48 h the expression of Tec protein was increased. Counter blots confirmed that the expression of Btk was restricted to the normal cells (Fig. 6 B). Next, the response of Tec kinase to LPS in M-CSF–treated monocytes was investigated using autokinase assays of immunoprecipitated enzyme. Like Btk, Tec kinase activity was increased in response to LPS treatment of human M-CSF–treated monocytes (Fig. 6 C).

Discussion

Our data has shown that stimulation of human monocytes with LPS triggers the activation of the nonreceptor tyrosine kinase, Btk. Moreover, in XLA monocytes that lack functional Btk, there is a failure to respond to LPS treatment as determined by their reduced TNFα production after stimulation. Our initial findings led us to further examine the contribution of Btk in controlling TNFα production. Adenoviral gene transfer has been used extensively to investigate the role of different transgenes in primary cells due to the ability of adenoviruses to infect both quiescent and dividing cells at high efficiency (4). Overexpression of Btk resulted in a consistent two- to threefold increase in TNFα production from M-CSF monocytes. In B cells, activation of the NF-κB transcription complex by signals derived from the B cell antigen receptor act via Btk to control B cell development, survival, and antigenic responses. However, the actions of Btk in macrophages appear to be independent of NF-κB activation and there is no defect in IκBα degradation in response to LPS in XLA monocytes.

TNF biosynthesis is under the control of multiple and complex regulatory mechanisms. Because the Tec family is

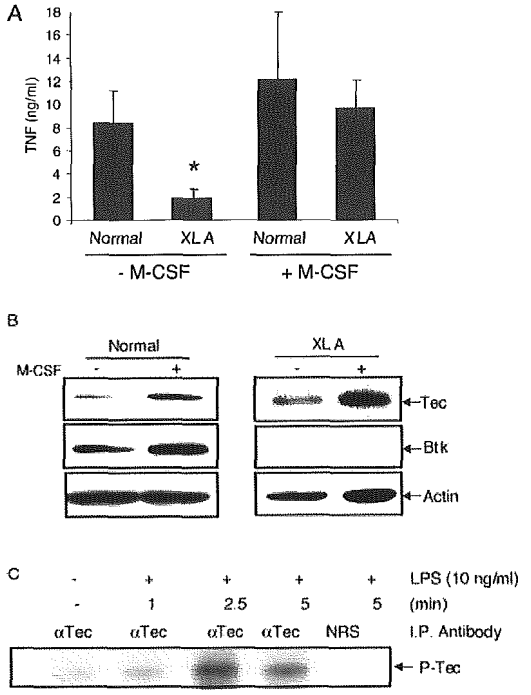

Figure 6. The effect of M-CSF treatment on LPS-stimulated TNFα production and Tec expression. (A) Adherent monocytes from XLA and normal donors were either stimulated with LPS for 2 h, or incubated with M-CSF for 48 h before LPS stimulation for 2 h. Supernatants were assayed for TNFα production. (B) Adherent monocytes from normal (lanes 1 and 2) and XLA donors (lanes 3 and 4) were either lysed immediately, or after M-CSF treatment for 48 h. Western blot analysis was performed using either α-TecSH3, α-Btk, or α-actin antibody. (C) Elutriated monocytes from normal donors were stimulated with LPS for the indicated time periods. Tec was immunoprecipitated and in vitro autokinase assay was performed. Each study is representative of at least three separate experiments.

known to interact with a wide range of signal transduction molecules (18), we took the alternate approach of examining the effect of Btk on the UTRs of TNFα. Using the 5′ promoter-luciferase and 5′ promoter-luciferase-3′ UTR adenoviral reporter constructs, we were able to show that the ability of Btk to enhance TNFα production required the 3′ UTR. There is considerable evidence indicating that some of these may occur at the translational level and be mediated by AU-rich elements (AREs) in the 3′ UTR of the mRNA. Certain inflammatory gene mRNAs, including cyclooxygenase-2, IL-6, IL-8, and TNFα mRNAs, are stabilized by activation of the p38 MAPK pathway by stimuli such as IL-1 and LPS (37, 41–43). Studies with mRNA reporter constructs have shown that the p38 MAPK-mediated stabilization directly involves AREs (38). Thus, AREs confer instability on mRNAs. However, after activation of the p38 MAPK pathway, they allow mRNA stabilization and hence increased protein expression. There is also a strong association between Btk and p38 MAPK in B cells showing that the activation of p38 MAPK was completely inhibited in cells deficient in Lyn and Btk, and the introduction of wild-type Btk, but not kinase-inactive Btk, restored the p38 MAPK activation in response to 280 nm UV irradiation in chicken DT40 B cells (44). The precise regions of the TNF 3′ UTR involved in this interaction with Btk and the potential involvement of p38 MAPK and other intermediary molecules is a field of ongoing research in our laboratory.

The proposition that Btk is essential for LPS-induced TNFα production is not easily reconciled with the XLA phenotype that shows no obvious gross defect of the innate immune system. However, there have been limited reports that XLA patients have reduced inflammatory responses (45). This is in contrast to patients with common variable immunodeficiency who are prone to multiorgan granulomatous disease, although they too have a type of antibody deficiency similar to the XLA patients (28, 46). In humans, Btk is absolutely required for the progression of developing B cells through the pro-B to pre-B stage. However, in *xid* mice the absence of Btk alone does not result in the same phenotype and it is only when Tec is also ablated that the same B cell deficiency is observed (40). It would be of interest to investigate LPS responsiveness in monocyte/macrophages from these mice. This suggests that Tec might be able to substitute for the absence of Btk in mouse pro-B cells, but at this stage of development in man, Tec is either unavailable or is incapable of substituting for Btk (47). It is of interest to note that monocyte differentiation toward macrophages ablates the differences observed between the XLA patients and normal donors (Fig. 6 A) and that this is accompanied by an increase in Tec levels (Fig. 6 B). The observation that Tec kinase is expressed in resting monocytes from XLA and normal individuals, although at a lower level, may explain why there is some response to LPS in the Btk-deficient cells. The data obtained here would suggest that without an increase in Tec kinase expression induced by M-CSF, there is insufficient kinase activity in the resting XLA monocytes to support a full LPS response. This hypothesis is supported by the observation that at the lowest LPS concentration used in this study (0.1 ng/ml), TNFα production by XLA and normal cells was similar (Fig. 1 A). The majority of the studies in mice (23, 24), with the exception of the study by Mukhopadhyay et al. (25), have been unable to find any differences in LPS responsiveness between *xid* and normal macrophages. We also examined the responsiveness of peritoneal macrophages from *xid* mice versus normal mice and were unable to observe any differences in TNFα production and NF-κB DNA binding activity in response to LPS (unpublished data). Taken together, these data suggest that rather than a difference between murine and human cells, that it is in fact a difference between monocytes and macrophages. It is therefore possible that the up-regulation of Tec, or other Tec kinase family members, in human macrophages may explain why there is no major impairment of innate immunity in XLA patients although further work is required to confirm this hypothesis.

In summary, this study has demonstrated that Btk is not only another tyrosine kinase activated by LPS, but also that deficiency in its expression is associated with impairment of

TNFα expression. Furthermore, overexpression of Btk in macrophages synergizes with LPS to induce TNFα production by stabilizing TNFα mRNA. Although these data imply that Btk is the first described tyrosine kinase having a key role in LPS-induced production of TNFα by monocytes, this role is probably not restricted to Btk alone. The intriguing question remains as to what role Tec kinases may have in mediating TNFα production by myeloid cells to other stimuli, particularly those involved in inflammatory conditions like rheumatoid arthritis and Crohn's disease, where TNFα is a validated therapeutic target.

The authors would like to thank Dr. V. Tybulewicz and Ms. L. Vanes (National Institute for Medical Research, Millhill, United Kingdom) for providing access to the *xid* mice. Many thanks to Prof. C. Kinnon and Dr. M. Tomlinson for providing access to the Btk and Tec family antibodies used in this study. The authors would also like to thank Dr. A. Clark for constructive criticism of the manuscript.

N.J. Horwood is a Howard Florey Research Fellow. T. Mahon is a Training and Mobility of Researchers Marie Curie Fellow. These studies were supported by a block grant from the Arthritis Research Campaign, UK.

Submitted: 22 October 2002
Revised: 11 February 2003
Accepted: 11 March 2003

References

1. Feldmann, M., F.M. Brennan, and R.N. Maini. 1996. Rheumatoid arthritis. *Cell.* 85:307–310.
2. Beutler, B., and A. Cerami. 1988. Tumor necrosis, cachexia, shock, and inflammation: a common mediator. *Annu. Rev. Biochem.* 57:505–518.
3. Bondeson, J., B. Foxwell, F. Brennan, and M. Feldmann. 1999. Defining therapeutic targets by using adenovirus: blocking NF-kappaB inhibits both inflammatory and destructive mechanisms in rheumatoid synovium but spares anti-inflammatory mediators. *Proc. Natl. Acad. Sci. USA.* 96:5668–5673.
4. Foxwell, B., K. Browne, J. Bondeson, C. Clarke, R. de Martin, F. Brennan, and M. Feldmann. 1998. Efficient adenoviral infection with IkappaB alpha reveals that macrophage tumor necrosis factor alpha production in rheumatoid arthritis is NF-kappaB dependent. *Proc. Natl. Acad. Sci. USA.* 95:8211–8215.
5. Lee, J.C., J.T. Laydon, P.C. McDonnell, T.F. Gallagher, S. Kumar, D. Green, D. McNulty, M.J. Blumenthal, J.R. Heys, S.W. Landvatter, et al. 1994. A protein kinase involved in the regulation of inflammatory cytokine biosynthesis. *Nature.* 372:739–746.
6. Kotlyarov, A., A. Neininger, C. Schubert, R. Eckert, C. Birchmeier, H.D. Volk, and M. Gaestel. 1999. MAPKAP kinase 2 is essential for LPS-induced TNF-alpha biosynthesis. *Nat. Cell Biol.* 1:94–97.
7. Novogrodsky, A., A. Vanichkin, M. Patya, A. Gazit, N. Osherov, and A. Levitzki. 1994. Prevention of lipopolysaccharide-induced lethal toxicity by tyrosine kinase inhibitors. *Science.* 264:1319–1322.
8. Geng, Y., B. Zhang, and M. Lotz. 1993. Protein tyrosine kinase activation is required for lipopolysaccharide induction of cytokines in human blood monocytes. *J. Immunol.* 151:6692–6700.
9. Han, J., J.D. Lee, P.S. Tobias, and R.J. Ulevitch. 1993. Endotoxin induces rapid protein tyrosine phosphorylation in 70Z/3 cells expressing CD14. *J. Biol. Chem.* 268:25009–25014.
10. Weinstein, S.L., J.S. Sanghera, K. Lemke, A.L. DeFranco, and S.L. Pelech. 1992. Bacterial lipopolysaccharide induces tyrosine phosphorylation and activation of mitogen-activated protein kinases in macrophages. *J. Biol. Chem.* 267:14955–14962.
11. Knapp, K.M., and B.K. English. 2000. Ceramide-mediated stimulation of inducible nitric oxide synthase (iNOS) and tumor necrosis factor (TNF) accumulation in murine macrophages requires tyrosine kinase activity. *J. Leukoc. Biol.* 67: 735–741.
12. Stefanova, I., M.L. Corcoran, E.M. Horak, L.M. Wahl, J.B. Bolen, and I.D. Horak. 1993. Lipopolysaccharide induces activation of CD14-associated protein tyrosine kinase p53/56lyn. *J. Biol. Chem.* 268:20725–20728.
13. Beaty, C.D., T.L. Franklin, Y. Uehara, and C.B. Wilson. 1994. Lipopolysaccharide-induced cytokine production in human monocytes: role of tyrosine phosphorylation in transmembrane signal transduction. *Eur. J. Immunol.* 24:1278–1284.
14. Crowley, M.T., S.L. Harmer, and A.L. DeFranco. 1996. Activation-induced association of a 145-kDa tyrosine-phosphorylated protein with Shc and Syk in B lymphocytes and macrophages. *J. Biol. Chem.* 271:1145–1152.
15. Crowley, M.T., P.S. Costello, C.J. Fitzer-Attas, M. Turner, F. Meng, C. Lowell, V.L. Tybulewicz, and A.L. DeFranco. 1997. A critical role for Syk in signal transduction and phagocytosis mediated by Fcgamma receptors on macrophages. *J. Exp. Med.* 186:1027–1039.
16. Meng, F., and C.A. Lowell. 1997. Lipopolysaccharide (LPS)-induced macrophage activation and signal transduction in the absence of Src-family kinases Hck, Fgr, and Lyn. *J. Exp. Med.* 185:1661–1670.
17. Williams, L.M., and A.J. Ridley. 2000. Lipopolysaccharide induces actin reorganization and tyrosine phosphorylation of Pyk2 and paxillin in monocytes and macrophages. *J. Immunol.* 164:2028–2036.
18. Takesono, A., L.D. Finkelstein, and P.L. Schwartzberg. 2002. Beyond calcium: new signaling pathways for Tec family kinases. *J. Cell Sci.* 115:3039–3048.
19. Smith, C.I., B. Baskin, P. Humire-Greiff, J.N. Zhou, P.G. Olsson, H.S. Maniar, P. Kjellen, J.D. Lambris, B. Christensson, L. Hammarstrom, et al. 1994. Expression of Bruton's agammaglobulinemia tyrosine kinase gene, BTK, is selectively down-regulated in T lymphocytes and plasma cells. *J. Immunol.* 152:557–565.
20. Desiderio, S. 1997. Role of Btk in B cell development and signaling. *Curr. Opin. Immunol.* 9:534–540.
21. Huber, B., and F. Melchers. 1979. Frequencies of mitogen-reactive B cells in the mouse. Lipopolysaccharide-, lipoprotein- and Nocardia mitogen-reactive B cells in CBA/N mice. *Eur. J. Immunol.* 9:827–829.
22. Scher, I. 1982. The CBA/N mouse strain: an experimental model illustrating the influence of the X-chromosome on immunity. *Adv. Immunol.* 33:1–71.
23. Zhao, Y.X., A. Abdelnour, R. Holmdahl, and A. Tarkowski. 1995. Mice with the xid B cell defect are less susceptible to developing Staphylococcus aureus-induced arthritis. *J. Immu-*

nol. 155:2067–2076.
24. Hata, D., Y. Kawakami, N. Inagaki, C.S. Lantz, T. Kitamura, W.N. Khan, M. Maeda-Yamamoto, T. Miura, W. Han, S.E. Hartman, et al. 1998. Involvement of Bruton's tyrosine kinase in FcepsilonRI-dependent mast cell degranulation and cytokine production. *J. Exp. Med.* 187:1235–1247.
25. Mukhopadhyay, S., M. Mohanty, A. Mangla, A. George, V. Bal, S. Rath, and B. Ravindran. 2002. Macrophage effector functions controlled by Bruton's tyrosine kinase are more crucial than the cytokine balance of T cell responses for microfilarial clearance. *J. Immunol.* 168:2914–2921.
26. Golding, B., H. Golding, P.G. Foiles, and J.I. Morton. 1983. CBA/N X-linked defect delays expression of the Y-linked accelerated autoimmune disease in BXSB mice. *J. Immunol.* 130:1043–1046.
27. Jansson, L., and R. Holmdahl. 1993. Genes on the X chromosome affect development of collagen-induced arthritis in mice. *Clin. Exp. Immunol.* 94:459–465.
28. Webster, A.D.B. 2001. Humoral immunodeficiencies. *In* Immunology and Allergy Clinics of North America. C.M. Roifman, editor. MD Consult (Elsevier), St. Louis, MO. 1–34.
29. He, T.C., S. Zhou, L.T. da Costa, J. Yu, K.W. Kinzler, and B. Vogelstein. 1998. A simplified system for generating recombinant adenoviruses. *Proc. Natl. Acad. Sci. USA.* 95: 2509–2514.
30. Denys, A., I.A. Udalova, C. Smith, L.M. Williams, C.J. Ciesielski, J. Campbell, C. Andrews, D. Kwaitkowski, and B.M. Foxwell. 2002. Evidence for a dual mechanism for IL-10 suppression of TNF-alpha production that does not involve inhibition of p38 mitogen-activated protein kinase or NF-kappa B in primary human macrophages. *J. Immunol.* 168:4837–4845.
31. Sanlioglu, S., C.M. Williams, L. Samavati, N.S. Butler, G. Wang, P.B. McCray, Jr., T.C. Ritchie, G.W. Hunninghake, E. Zandi, and J.F. Engelhardt. 2001. Lipopolysaccharide induces Rac1-dependent reactive oxygen species formation and coordinates tumor necrosis factor-alpha secretion through IKK regulation of NF-kappa B. *J. Biol. Chem.* 276: 30188–30198.
32. Mano, H., Y. Yamashita, K. Sato, Y. Yazaki, and H. Hirai. 1995. Tec protein-tyrosine kinase is involved in interleukin-3 signaling pathway. *Blood.* 85:343–350.
33. Vihinen, M., P.T. Mattsson, and C.I.E. Smith. 1997. BTK, the tyrosine kinase affected in X-linked agammaglobulinemia. *Front. Biosci.* 2:d27–d42.
34. Cambronero, R., W.A. Sewell, M.E. North, A.D. Webster, and J. Farrant. 2000. Up-regulation of IL-12 in monocytes: a fundamental defect in common variable immunodeficiency. *J. Immunol.* 164:488–494.
35. Yoza, B.K., J.Y. Hu, and C.E. McCall. 1996. Protein-tyrosine kinase activation is required for lipopolysaccharide induction of interleukin 1beta and NFkappaB activation, but not NFkappaB nuclear translocation. *J. Biol. Chem.* 271: 18306–18309.
36. Delude, R.L., M.J. Fenton, R. Savedra, Jr., P.Y. Perera, S.N. Vogel, R. Thieringer, and D.T. Golenbock. 1994. CD14-mediated translocation of nuclear factor-kappa B induced by lipopolysaccharide does not require tyrosine kinase activity. *J. Biol. Chem.* 269:22253–22260.
37. Rutault, K., C.A. Hazzalin, and L.C. Mahadevan. 2001. Combinations of ERK and p38 MAPK inhibitors ablate tumor necrosis factor-alpha (TNF-alpha) mRNA induction. Evidence for selective destabilization of TNF-alpha transcripts. *J. Biol. Chem.* 276:6666–6674.
38. Brook, M., G. Sully, A.R. Clark, and J. Saklatvala. 2000. Regulation of tumour necrosis factor alpha mRNA stability by the mitogen-activated protein kinase p38 signalling cascade. *FEBS Lett.* 483:57–61.
39. Tomlinson, M.G., T. Kurosaki, A.E. Berson, G.H. Fujii, J.A. Johnston, and J.B. Bolen. 1999. Reconstitution of Btk signaling by the atypical tec family tyrosine kinases Bmx and Txk. *J. Biol. Chem.* 274:13577–13585.
40. Ellmeier, W., S. Jung, M.J. Sunshine, F. Hatam, Y. Xu, D. Baltimore, H. Mano, and D.R. Littman. 2000. Severe B cell deficiency in mice lacking the tec kinase family members Tec and Btk. *J. Exp. Med.* 192:1611–1624.
41. Dean, J.L., M. Brook, A.R. Clark, and J. Saklatvala. 1999. p38 mitogen-activated protein kinase regulates cyclooxygenase-2 mRNA stability and transcription in lipopolysaccharide-treated human monocytes. *J. Biol. Chem.* 274:264–269.
42. Winzen, R., M. Kracht, B. Ritter, A. Wilhelm, C.Y. Chen, A.B. Shyu, M. Muller, M. Gaestel, K. Resch, and H. Holtmann. 1999. The p38 MAP kinase pathway signals for cytokine-induced mRNA stabilization via MAP kinase-activated protein kinase 2 and an AU-rich region-targeted mechanism. *EMBO J.* 18:4969–4980.
43. Wang, S.W., J. Pawlowski, S.T. Wathen, S.D. Kinney, H.S. Lichenstein, and C.L. Manthey. 1999. Cytokine mRNA decay is accelerated by an inhibitor of p38-mitogen-activated protein kinase. *Inflamm. Res.* 48:533–538.
44. Kabuyama, Y., M.K. Homma, T. Kurosaki, and Y. Homma. 2002. Early signaling events induced by 280-nm UV irradiation. *Eur. J. Biochem.* 269:664–670.
45. Webster, A.D.B. 1978. Mycoplasma osteomyelitis and pneumonia associated with primary hypogammaglobulinaemia. *Skeletal Radiolog.* 3:131–132.
46. Smith, C.I.E., and O.N. Witte. 1998. Primary Immunodeficiency Diseases: A Molecular and Genetic Approach. H. Ochs, C.D.E. Smith, and J. Puck, editors. Oxford University Press, Oxford. 263–284.
47. Pillai, S., and S.T. Moran. 2002. Tec kinase pathways in lymphocyte development and transformation. *Biochim. Biophys. Acta.* 1602:162–167.

CYTOKINE
www.elsevier.com/locate/jnlabr/ycyto
Cytokine 24 (2003) 36–45

Function of a conserved residue in the amino terminal α-helix of four helical bundle cytokines

Yasuo Oshima*, Akio Fujimura

Department of Clinical Pharmacology, Jichi Medical School, Tochigi 329-0498, Japan

Received 11 April 2003; received in revised form 31 May 2003; accepted 2 July 2003

Abstract

The Glu residue in the helix A is conserved among many cytokines. Mutation in this residue converts some cytokines to an antagonist. Such an artificial cytokine with an antagonist activity may be useful in a clinical area. In this study we generated a mutant granulocyte colony-stimulating factor (G-CSF) termed G-CSF.E20K in which this residue is substituted to Lys. It is known that G-CSF binds to a homodimeric receptor, while other cytokines which can be converted to antagonists bind to heterodimeric receptors. We showed that G-CSF.E20K does not bind to the receptor at all, and that it fails to stimulate proliferation. Thus, the mutant did not act as an antagonist. We propose that the nature of the receptor, namely whether it is a homodimer or heterodimer, determines the antagonist activity of the mutant.

Keywords: α-Helix; Amino acid residue; Ligand–receptor interaction; Mutein; Recombinant protein

Abbreviations: IL, interleukin; G-CSF, granulocyte colony-stimulating factor; GM-CSF, granulocyte macrophage colony-stimulating factor; wt, wild-type

1. Introduction

Adequate cytokine activity is critical for the maintenance of body homeostasis including hematopoiesis and immune status. It is not surprising that the malfunction of cytokine activity is linked to many human diseases. Consequently, under the conditions of inappropriately high or low cytokine activity, cytokine antagonists or agonists may constitute valuable families of new therapeutic agents [1–5]. Actually some wild-type ligands or biotechnologically modified cytokines have been widely used in clinical practice [6,7]. Recently it is getting more common to create a new bioactive molecule using three-dimensional structure information with a computer-aided drug design system. These methods have been successful in some areas such as protein tyrosine phosphatase inhibitors and tyrosine kinase inhibitors [8–11]. Quality of a designed molecular seed is mainly dependent on an information of structure–function relationship in atomic level. Although the structure–function relationship was largely analyzed in each cytokine, information generalized in each family was limited. Insight of active sites such as active motifs or binding interfaces may help to design a novel agonistic or antagonistic small molecule to cytokine receptors.

Most of four helical bundle cytokine molecules conserved negatively charged Glu residue at the amino terminal α-helix (helix A). The conserved Glu locates at the identical position if aligned based on the pattern of hydrophobic residues of the first α-helices [12,13]. Seven antagonistic molecules have been created by substituting the conserved Glu into the positively charged Lys residue [12]. While these antagonists bind to their specific receptor, they do not stimulate any signal transductions that trigger a cell proliferation or the other functions even at high concentration. Both conserved Glu of human interleukin-4 and human granulocyte colony-stimulating

* Corresponding author. Tel.: +81-285-58-7388; fax: +81-285-44-7562.
E-mail address: oshima@jichi.ac.jp (Y. Oshima).

1043-4666/03/$ - see front matter © 2003 Elsevier Ltd. All rights reserved.
doi:10.1016/S1043-4666(03)00268-0

factor (G-CSF), in which the crystal structure of the ligand–receptor complex is clarified, exist at the binding interface [14,15]. As far as we explore three-dimensional structures of their ligand–receptor complex, their conserved Glu form hydrogen bonds with Tyr residues of their receptor molecules. Moreover, some of neutralizing antibodies against human G-CSF receptor recognize epitopes including the conserved Tyr residue [16]. These observations led us to speculate that substituting the Glu of human G-CSF may create a novel G-CSF antagonist. In this study, we created a novel mutant G-CSF termed G-CSF.E20K and tested its biological activities.

2. Results and discussions

2.1. Alignment of amino terminal helices of cytokines

The binding of cytokines to their functional receptors and subsequent signal transduction is a complex process which includes the interaction with multiple receptor molecules. Many cytokines have overall conserved structure as four major α-helical bundles. Many efforts have been made to determine amino acid residues which govern receptor binding and signal transduction for many cytokines [14,17–36]. A part of amino acid sequence of helix A is shown in Table 1. Homology alignment based on the locations of hydrophobic residues (underlined) indicates that there is an absolute conservation of a negatively charged residue (Glu/Asp) in the helix A (Table 1). This conserved residue may have a conserved function.

2.2. Location of the conserved residues

Helices A are shown in three-dimensional structures (Fig. 1A). It is shown that there is a cluster of hydrophobic residues at one side of each helix A and that the conserved negatively charged residue locates at another side of the hydrophobic residues. These hydrophobic residues make a hydrophobic core in each protein and may play some roles in keeping its conformation. On the other hand, the conserved negatively charged residues are exposed to solvent and may interact with polar or ionic molecules surrounding the protein. Human G-CSF [15] and human interleukin-4 [14] are analyzed as a complex with their specific receptor chains. The conserved Glu of these cytokines locates at binding interface where the side chains of approximately 15 amino acid residues locate close to receptor molecules and indicate van der Waals contacts (within 4.2 Å). The conserved Glu of G-CSF and interleukin-4 exist approximately 2.7–2.9 Å from Tyr residues of the receptor chains and form hydrogen bonds with the Tyr residues (Fig. 1B). The conserved residues may have a conserved role in a ligand–receptor interaction.

Table 1
Multiple alignment of helix A

Cytokine	Amino acid sequence	Determined helix A	(PDB ID)
hIL-2	LLL **D** LQMIL	Thr7 (Lys9)~Ile28	(3INK)
hIL-3	SIVK **E** IIGKL	Ile5~His12	(1JLI)
hIL-4	ITLQ **E** IIKTL	Ile5~Thr18	(1IAR)
hIL-5	ALVK **E** TLALLSTH	Thr3~His17	(1HUL)
vIL-6	WVID **E** CFRDLCYR	Lys9~Arg33	(1I1R)
hIL-6	RYIL **E** GISALRK	Ser23~Ser49	(1ALU)
hIL-10	NMLR **D** LRDAFS	Pro20~Phe30	(1J7V)
vIL-10	QMLR **D** LRDAFS	Arg10~Val19	(1VLK)
hIL-13	ALR **E** LIEEL	Ala9~Thr21	(1GA3)
hEPO	LEAK **E** AENITTG	Glu13~Thr26	(1EER)
dG-CSF	LKCL **E** QMRKV	Gln12~Thr39	(1BGD)
bG-CSF	LKCL **E** QVRKI	Gln11~Ala38	(1BGC)
hG-CSF	LKCL **E** QVRKI	Gln12~Thr39	(1CD9)
hGM-CSF	NAIQ **E** ARRLLNL	Trp13~Leu28	(1CSG)

The amino acid sequences of amino terminal helix of cytokines (helix A) are aligned as mentioned in Section 3 based on the position of hydrophobic residues (underlined). The amino acid residues, which compose helix A, were determined by three-dimensional coordinates registered in the Brookhaven Protein Data Bank (http://www.rcsb.org/pdb/). Numbering of amino acid residues is based on the coordinate file, which may or may not differ from experimentally determined amino acid residue numbering. Parts of the helix A are shown in the table. Protein Data Bank ID (PDB ID) of each protein is shown in the table too. There are conserved negatively charged residues, E (Glu) or D (Asp) (bold characters) at the identical location. Abbreviation in the table of amino acid residues is followed by standard one letter symbol. Other abbreviations are as follows: h, *Homo sapiens*; v, virus; d, *Canis familiaris*; b, *Bos taurus*; IL, interleukin; EPO, erythropoietin; G-CSF, granulocyte colony-stimulating factor; GM-CSF, granulocyte macrophage colony-stimulating factor.

2.3. Purified wtG-CSF and G-CSF.E20K

G-CSF.E20K and wtG-CSF were produced in prokaryotic expression system as mentioned in Section 3. As a nature of these expression systems, the expressed proteins have additional Met residue at the amino terminus of the desired peptides in order to create translation-initiation codon 'ATG'. The purified protein showed a prominent single band at approximately 14 kDa in Coomassie Blue-stained sodium dodecyl sulphate polyacrylamide gel (Fig. 2). Though there were still faint bands in some expressions, purity of these proteins was estimated to be better than 95% by visual inspection. Since we induced, refolded and purified both proteins in an identical manner, both proteins must have essentially same folding quality.

2.4. Bioactivities of the conserved residue in human G-CSF

We found an interesting matter in antagonistic muteins. The reported antagonists made by substituting the conserved residues are limited only in acting through the heterodimeric receptor system in which a ligand interacts with different receptor molecules to generate a signal transduction. For example, granulocyte macrophage

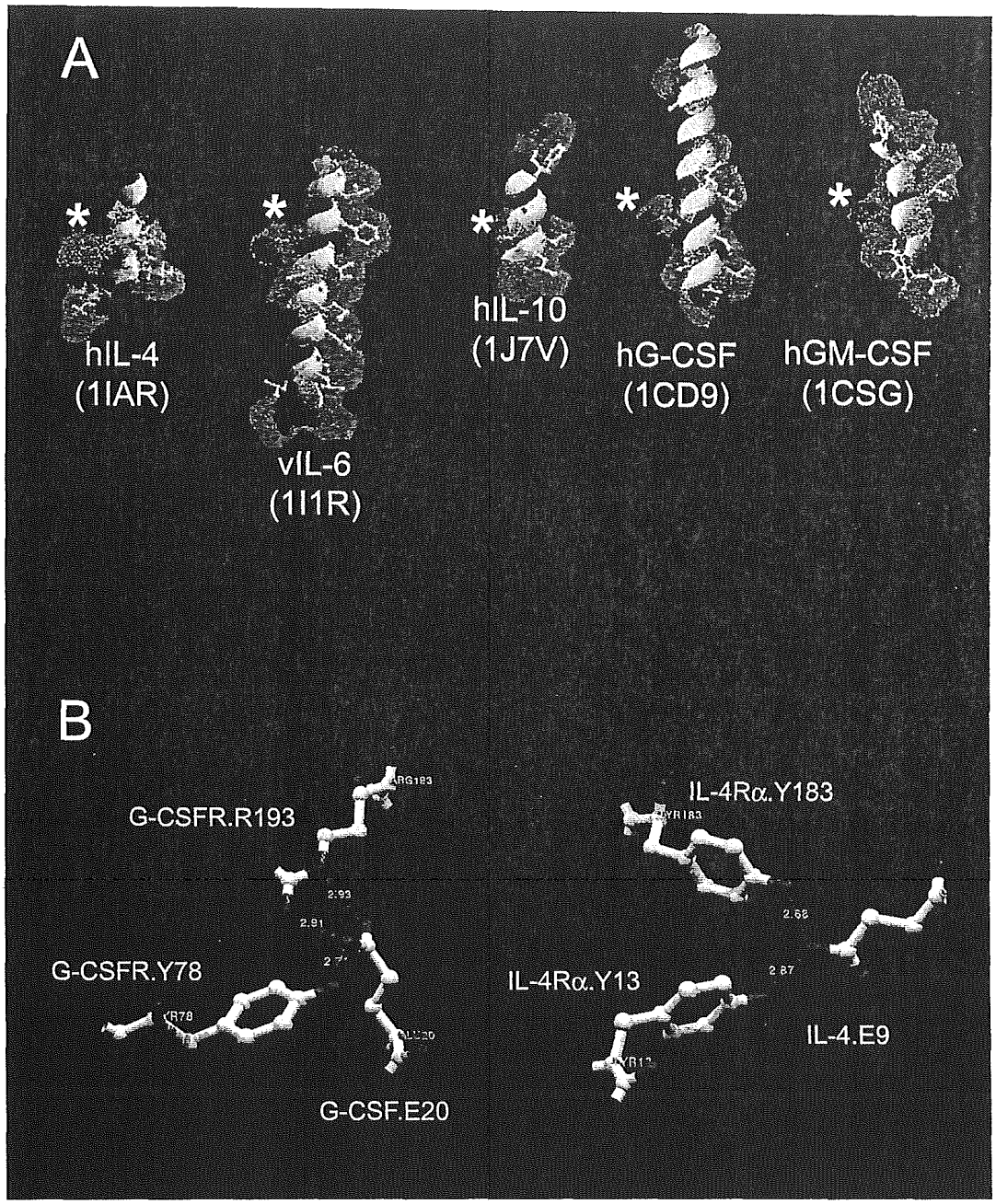

Fig. 1. Conserved structure of helix A. Three-dimensional structures of cytokines were shown in ribbon diagram (A) and ball and stick expression (B). Coordinates were downloaded from Brookhaven Protein Data Bank (http://www.rcsb.org/pdb/). Each PDB ID was shown in the figure. A. Helix A of hIL-4, vIL-6, hIL-10, hG-CSF and hGM-CSF is shown. Side chains of the negatively charged, conserved Glu were indicated by asterisks, and those of hydrophobic residues were shown in ball and stick expression and surrounded by gray surface area. The conserved residues are located at the other side of hydrophobic core in helix A of cytokines. B. The conserved Glu and side chains of receptor molecules are shown. Three-dimensional structures of the ligand–receptor complex indicated that the conserved Glu formed hydrogen bond with side chains of receptor molecules. Based on the three-dimensional structure of 20th amino acid Glu of hG-CSF, it forms hydrogen bond with 78th amino acid Tyr and 193rd amino acid Arg of the receptor molecule. Similarly, ninth amino acid Glu of hIL-4 forms hydrogen bond with 13th amino acid Tyr and 183rd amino acid Tyr. Together with these observations in this figure and previous reports that indicated importance of 78th amino acid Tyr of hG-CSF receptor, the conserved residues must be critically important for ligand–receptor interaction.

colony-stimulating factor (GM-CSF) utilizes two receptor molecules (GM-CSF receptor β chain and GM-CSF receptor α chain) to form the active high affinity ligand–receptor complex. The conserved residues exist in ligands not only for heterodimeric but also for homodimeric receptor systems. In this study, we analyzed biological function of the conserved residue of human G-CSF, which utilizes the homodimeric receptor system.

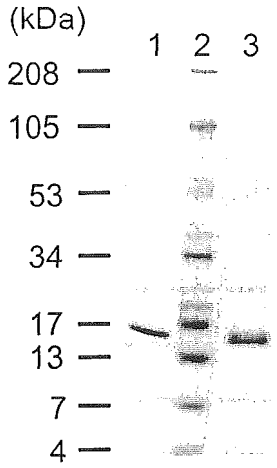

Fig. 2. Purified proteins. Expressed and purified protein was loaded on 10–20% gradient sodium dodecyl sulphate polyacrylamide gel, electrophoresed for 90 min at 130 V and then stained by the Coomassie Blue. Both wtG-CSF and G-CSF.E20K migrated at approximately 14 kDa and showed almost single band of target proteins. Though there were still faint bands in some expressions, purity of these proteins was estimated to be better than 95% by visual inspection. Lane 1, wtG-CSF; Lane 2, size marker, Multimark™ (Invitrogen); Lane 3, G-CSF.E20K.

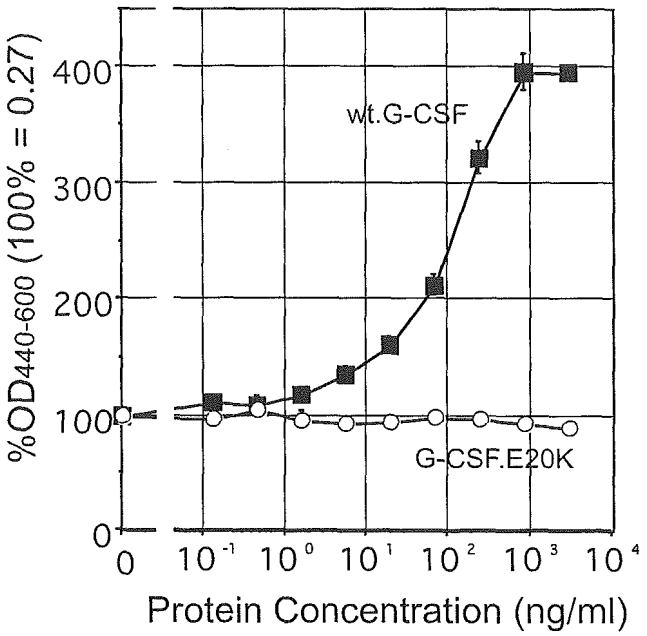

Fig. 3. Effect of wtG-CSF and G-CSF.E20K on proliferation of a leukemia cell line. UT-7/EPO G-full, a human myeloid leukemia cell line, which expresses human G-CSF receptors, was incubated at 37 °C with various concentrations of wtG-CSF (closed square) or G-CSF.E20K (open circle) as described in Section 3. Absorbance at 440 nm (A440) subtracted by absorbance at 600 nm (A600) is calculated as indicator of the formazan formation. Data are presented as mean percentage absorbance of quadruplicate determinants ± S.D. The wtG-CSF stimulated cell proliferation in a concentration-dependent manner while G-CSF.E20K did not. These assays were repeated for a few times.

As shown in Fig. 2, refolded and purified mutein as well as wtG-CSF showed almost single band in Coomassie Blue-stained gel. We used these pure proteins for bioassays. To test the biological activities to stimulate cell proliferation, we performed cell proliferation assays using UT-7/EPO G-full cells which express active human G-CSF receptors [37]. While wtG-CSF stimulated UT-7/EPO G-full cells proliferation in a concentration-dependent manner, G-CSF.E20K did not (Fig. 3). We also tested their binding activity using biotin-labeled G-CSF, termed bio-G-CSF. As shown in Fig. 4, wtG-CSF competitively bound to the UT-7/EPO G-full cell in a concentration-dependent manner. Approximately 150 ng/ml wtG-CSF competed the half of maximal binding of 100 ng/ml bio-G-CSF. On the other hand, G-CSF.E20K did not compete any bio-G-CSF binding even at increasing concentrations as high as 10 μg/ml. Since wtG-CSF showed cell proliferation and cell binding in our assay, our system worked properly including expression and purification of proteins, proliferation assay, and binding assay. Thus, we concluded that the binding and cell proliferation activities did not exist in G-CSF.E20K.

2.5. Polymer formation study

As reported before, human G-CSF tends to form polymers, especially in neutral and basic condition [38]. In addition, two G-CSF molecules form a stable complex with dimerized receptor molecules [15]. We tested whether G-CSF.E20K effectively forms a polymer. As shown in Fig. 5, after the incubation of 10 μg/ml G-CSF.E20K or wtG-CSF in pH 7.4 at 4 °C for 16 h, these agents formed dimer or other polymers. The density of polymers seemed to be similar in both proteins. As expected, the polymerized G-CSF.E20K was reduced by 2-mercaptoethanol and migrated around 14 kDa. The G-CSF antigenicity in both polymer and monomer forms was confirmed by the Western blotting in both wtG-CSF and G-CSF.E20K (Fig. 5B). Thus, substituting the conserved Glu did not affect the polymer formation under this condition.

2.6. Function of the conserved residues

While seven molecules in which the conserved residues are substituted to Lys, have antagonistic activities [12], G-CSF.E20K did not show any antagonistic activity. The substitution of the conserved residue of human G-CSF completely nullified its binding. In the heterodimeric receptor system such as interleukin-5, GM-CSF and interleukin-13, antagonistic mutein may bind to one of receptor chains, but not another (Fig. 6B). Thus the muteins act as antagonists. On the other hand, in the homodimeric receptor system like G-CSF, the mutein may not bind to any receptor chain. Thus G-CSF.E20K did not bind to its receptors (Fig. 6C). In the early

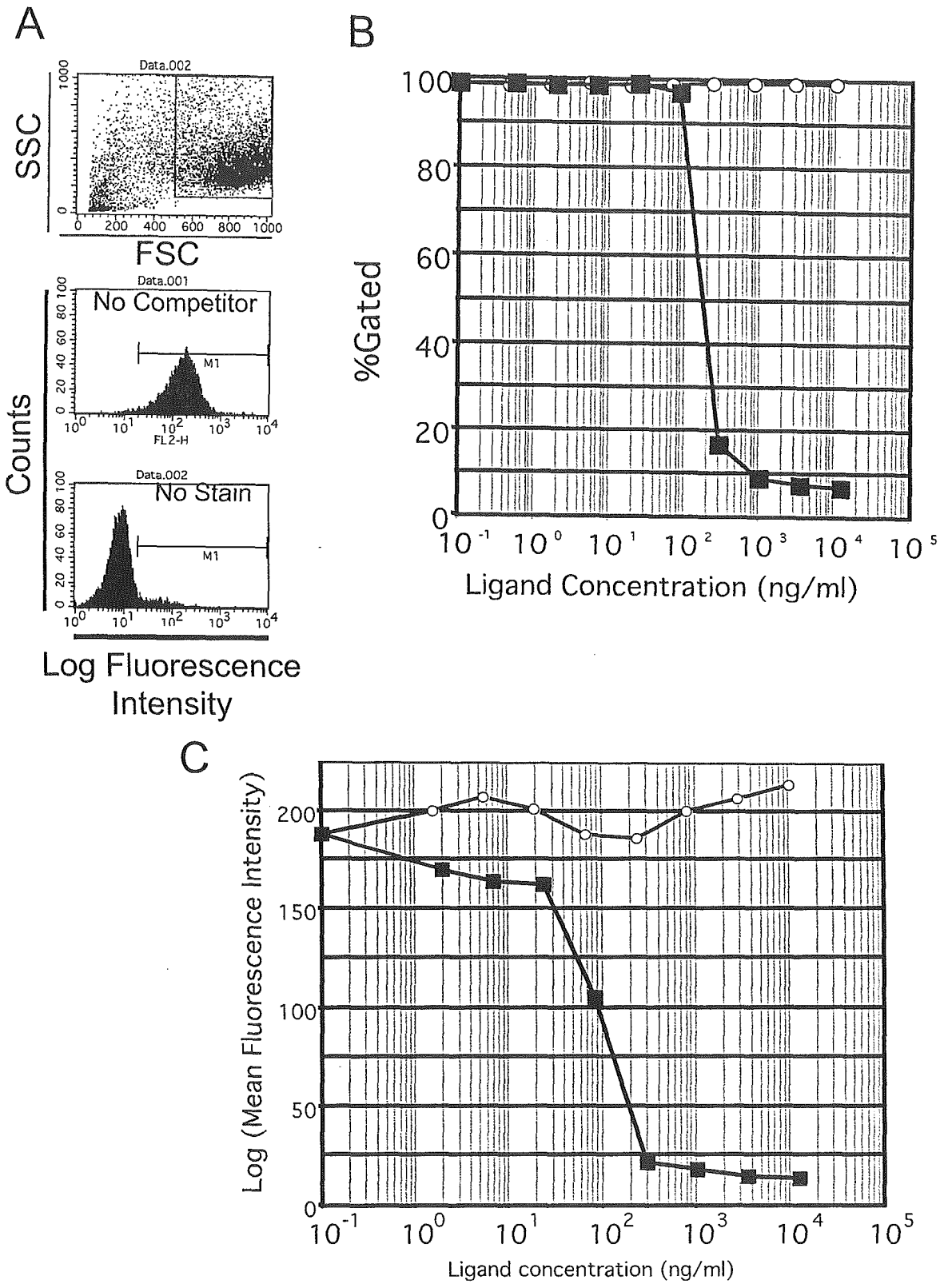
A
Data.002
SSC
FSC
Data.001
No Competitor
M1
Counts
FL2-H
Data.002
No Stain
M1
Log Fluorescence Intensity
B
%Gated
Ligand Concentration (ng/ml)
C
Log (Mean Fluorescence Intensity)
Ligand concentration (ng/ml)

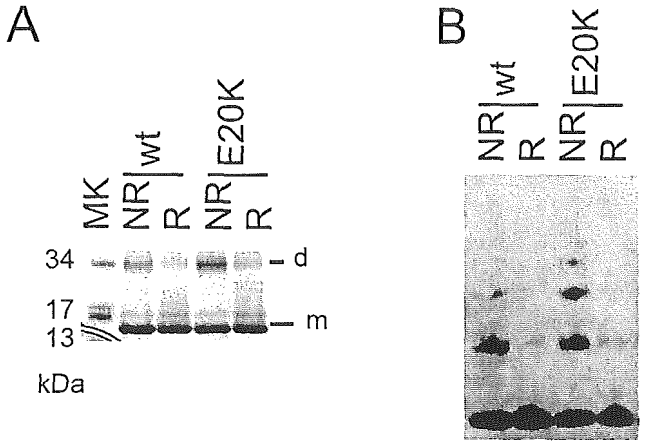

Fig. 5. Polymer formation of wtG-CSF and G-CSF.E20K. After the incubation at 4 °C for 16 h. 10 μg/ml protein was loaded on the SDS gel. Abbreviations: wt, wtG-CSF; E20K, G-CSF.E20K; MK, Multimark™ or molecular size marker; R, reduced condition; NR, non-reduced condition; m, indicates size of monomer G-CSF; d, indicates size of dimer. A. Both wtG-CSF and G-CSF.E20K showed dimer formation when they were electrophoresed under a non-reducing condition. On the other hand, under a reducing condition, the dimers were reduced and migrated to approximately 14 kDa, a size of monomer. B. G-CSF antigenicity of polymers of G-CSF.E20K and wtG-CSF were confirmed by Western blotting using anti-G-CSF polyclonal antibody.

reports it is indicated that wild-type growth hormone acts as an antagonist at high concentration [39,40]. As growth hormone ligand stimulates the signal transduction by forming 1 : 2 ligand–receptor complex, this antagonistic activity could be due to forming 1 : 1 ligand–receptor inactive complex (Fig. 6A). Such a phenomenon has never been reported for human G-CSF. Lack of antagonistic activity of wtG-CSF at high concentration may be due to its nature to form 2 : 2 ligand–receptor complex as a signaling complex (Fig. 6C).

3. Materials and methods

3.1. Multiple alignment and analysis of three-dimensional structures

Sequence analysis and multiple alignments were performed as described before [12,13,41,42]. To date, three-dimensional structures of at least 14 cytokines have been experimentally determined, including human interleukin-2 [43,44], human interleukin-3 [45], human interleukin-4 [46], human interleukin-5 [47], human herpesvirus-6 interleukin-6 [48], human interleukin-6 [49], human herpesvirus-4 interleukin-10 [50], human interleukin-10 [51], human interleukin-13 [52], human erythropoietin [53], *Canis familiaris* G-CSF [54], *Bos taurus* G-CSF [54], human G-CSF [15], and human GM-CSF [55]. Their fine structures including α-helix, loop, β-sheet, molecular surface and solvent accessibilities were analyzed using Swiss PDB viewer as described before [56].

3.2. Materials

Restriction endonucleases and DNA ligase were obtained from Takara Co. Ltd. (Shiga, Japan). Fast protein liquid chromatographic (FPLC) columns and S-sepharose FF were purchased from Pharmacia (Piscataway, NJ). Advantage-HF polymerase chain reaction (PCR) kit was from Clontech (Palo Alto, CA). The pET based expression vector with ampR gene was used for construction of mutein clone. Plasmids were amplified in *Escherichia coli* (DH5α high efficiency transformation) (GIBCO BRL Life Technology, Grand Island, NY) and extracted using Qiagen spin kits (Chatsworth, CA). UT-7/EPO G-full, human leukemia cell line, was kindly gifted from Dr. Komatsu (Jichi Medical School, Japan). The UT-7/EPO G-full cells express human G-CSF receptor and proliferate by human G-CSF in dose-dependent manner, were grown under human G-CSF [37].

3.3. Construction of plasmids encoding wtG-CSF and G-CSF.E20K

The mutagenesis of G-CSF gene was performed using a cDNA of wild-type G-CSF(wtG-CSF) as a template using sense primer 5′-taa cat atg acc ccg ctg ggc ccg gcg agc agc ctg ccg cag agc ttt ctg ctg aaa tgc ctg aaa caa gtg cgt aag at-3′, anti-sense primer 5′-taa gaa ttc tca ggg ctg ggc aag gtg gcg tag-3′ in order to mutate Glu 20 to Lys (E20K) and to incorporate *NdeI* and *EcoRI* restriction enzyme sites at 5′- and 3′-termini, respectively. Similarly, sense primer 5′-taa cat atg acc ccg ctg ggc ccg gcg agc agc

Fig. 4. Binding study of wtG-CSF and G-CSF.E20K. A. One million per tube UT-7/EPO G-full cells were incubated with (no competitor) or without (no stain) 100 ng/ml biotin-labeled wtG-CSF (bio-G-CSF) [57,58] for 50 min at 4 °C. Washed cells were then incubated with phycoerythrin labeled streptavidin. Cell bound bio-G-CSF was detected as fluorescence intensity of phycoerythrin. Non-specific bindings of streptavidin–phycoerythrin without bio-G-CSF (lower panel) were minimal and stained cells with bio-G-CSF and streptavidin–phycoerythrin showed a significant increase in fluorescence intensities. B. UT-7/EPO G-full cells were incubated under the same condition except for the existence of various concentrations of G-CSF.E20K or wtG-CSF during the first incubation. G-CSF.E20K did not seem to affect fluorescence intensity or number of cell bound bio-G-CSF while wtG-CSF did. The percentage of gated cells was plotted. The only 150 ng/ml wt G-CSF (closed square) suppressed approximately 50% of gated cells. G-CSF.E20K (open circle) did not suppress the percentage of gated cells up to 10 μg/ml. C. This panel also shows another aspect of the result. Mean fluorescence intensity (MFI) was indicated. Approximately 100 ng/ml wtG-CSF (closed square) suppressed half of maximal MFI but G-CSF.E20K did not even in high concentration. These assays were repeated twice and both indicated essentially same result.

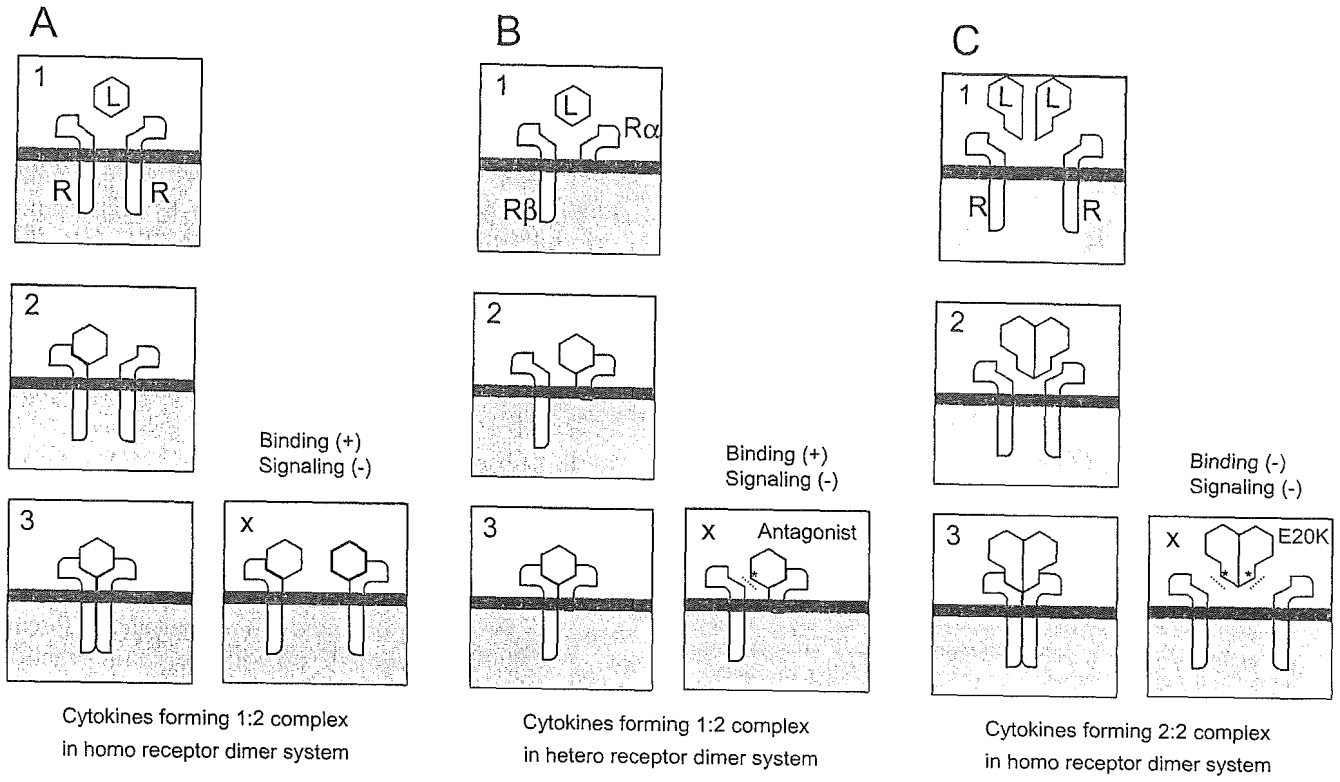

Fig. 6. Schematic diagram of a ligand–receptor interaction. A. One possible way of a ligand–receptor interaction in cytokine which forms 1 : 2 ligand–receptor signaling complex. This model was originally proposed by de Vos et al. in human growth hormone [40]. A ligand (shown as L in the figure) happens to come across, interacts and binds to an extracellular domain of a receptor molecule (shown as R) (A-2). Then the ligand and the receptor molecule form 1 : 1 complex without stimulating signal transduction. Then the complex interacts with another receptor molecule (R) on the cell surface membrane, and forms 1 : 2 signaling complex (A-3). High concentration of growth hormone is reported to act as antagonist [39]. This could be explained as follows: High concentration of growth hormone ligand occupies receptor molecule quickly and forms 1 : 1 complex as shown in (A-2). Since the complex is formed too fast to leave enough receptor molecules free in this case, signaling complex could not be formed effectively (A-x). B. An application of the previous model to heterodimeric receptor systems such as hIL-5, hGM-CSF and hIL-13. In these cytokines, a ligand interacts and forms primary complex with one particular receptor chain indicated as R.α (B-2). Then it interacts with another receptor chain (R.β) resulting in 1 : 2 signaling complex (B-3). Antagonists such as hIL-13.E13K, hGM-CSF.E21K and hIL-5.E13Q are considered to interact with first receptor chain (R.α) but mutation (shown as *) inhibits to interact with the second receptor chain (R.β) and to form 1 : 2 signaling complex. Thus these molecules occupy first receptor chains and act as antagonists (B-x). C. This model explains ligands which form 2 : 2 ligand–receptor signaling complex, such as human G-CSF. In this model, 1 : 1 ligand–receptor or ligand dimer may be formed (C-2) and thereafter, formed 2 : 2 ligand–receptor complex (C-3). In our case, G-CSF.E20K did not bind to receptor molecule even though they could effectively form dimer in neutral condition (C-x).

ctg ccg cag agc ttt ctg ctg aaa tgc ctg gaa caa gtg cgt aag at-3′, and anti-sense primer 5′-taa gaa ttc tca ggg ctg ggc aag gtg gcg tag-3′ were used to construct an expression vector for wtG-CSF. After subcloning the PCR products into pCR2.1® (Invitrogen, Carlsbad, CA), the plasmid was purified and digested with *NdeI* and *EcoRI*. The fragment was inserted into a prokaryotic pET based expression vector digested with same restriction enzymes. We confirmed the existence of the mutation and restriction sites by sequencing of the plasmids.

3.4. Expression and purification of recombinant proteins

Expression and purification of wtG-CSF and G-CSF.E20K were carried out by essentially similar techniques as previously reported [12,13,41]. The protein expression was induced by 1 mM IPTG. The wtG-CSF and G-CSF.E20K were produced in inclusion bodies. After washing, the inclusion bodies were solubilized using 7 M guanidine, refolded and purified by FPLC ion-exchange chromatography.

3.5. Cell proliferation assays

Proliferation assays were performed as described previously [42]. Briefly, UT-7/EPO G-full cells were washed twice with PBS to remove human G-CSF and then 5.0×10^3 cells per well were cultured in 96-well plates in Iscov's modified Dulbecco's medium containing 5% fetal bovine serum. Various concentrations of wtG-CSF and/or G-CSF.E20K were added to the wells, and the cells were cultured for approximately 2 days. Ten microliters WST-1 reagent (Takara Co. Ltd.) was added

to each well 4 h before the plates were read in an optical density reader, SpectroMAX340 (Molecular Devices Co. Ltd., Sunnyvale, CA). Assays were performed in quadruplicate and repeated at least twice. Absorbance at 440 nm (A440) and 600 nm (A600) per each well was read and A440–A600 is assumed to reflect the formazan production.

3.6. G-CSF receptor binding studies

Recombinant human G-CSF labeled with biotin (bio-G-CSF) was kindly provided from Dr. Tojo (Institutes of Medical Science, The University of Tokyo). The equilibrium binding studies were carried out as described elsewhere [57,58]. Briefly, 1×10^6 cells in 100 μl MACS/FACS buffer (phosphate buffered saline + 10% fetal bovine serum) were incubated at 4 °C for 50 min with bio-G-CSF (100 ng/ml) in the absence or presence of various concentration of unlabeled wtG-CSF or G-CSF.E20K. After washing with ice-cold MACS/FACS buffer, the cells in each tube were incubated with 90 μl containing 10 μl streptavidin–phycoerythrin (Becton Dickinson, San Jose, CA). After washing with ice-cold MACS/FACS buffer, the cell bound bio-G-CSF was determined by BD LSR™ (Becton Dickinson) as a fluorescence intensity of phycoerythrin. Data collection and statistical analysis have been done by CellQuest software (Becton Dickinson) according to the manufacturer's instruction.

3.7. Western blotting

Anti-human G-CSF goat polyclonal antibody was kindly provided by Dr. Tojo (Institutes of Medical Science, The University of Tokyo, Tokyo, Japan) and anti-goat immunoglobulin rabbit polyclonal antibody conjugated with horseradish peroxidase was purchased from Wako Pure Chemical Industries Ltd. (Osaka, Japan). Western blotting assays were performed by essentially similar techniques as reported before [12,13, 41,42]. Protein bound antibodies were detected with ECL (Pharmacia), the exposed X-ray films were developed and visualized as to the manufacturer's instruction.

3.8. Polymer formation study

To detect polymer formation of wtG-CSF or G-CSF.E20K, concentration of each protein was adjusted to 10 μg/ml in phosphate buffered saline pH 7.4 and incubated at 4 °C for 16 h. Then the protein was mixed with SDS loading buffer with or without 2-mercaptoethanol, incubated in boiling water for 5 min and analyzed by sodium dodecyl sulphate polyacrylamide gel electrophoresis. Proteins were visualized by Coomassie Blue stain as reported before.

Acknowledgements

We thank Drs. K. Sugimoto, S. Tsuruoka, M. Ohmori for valuable help in performing these studies. We also appreciate Drs. A. Tojo and N. Komatsu for providing biotin-labeled G-CSF and UT-7/EPO G-full cells, respectively.

References

[1] Dong F, Pouwels K, Hoefsloot LH, Rozemuller H, Lowenberg B, Touw IP. The C-terminal cytoplasmic region of the granulocyte colony-stimulating factor receptor mediates apoptosis in maturation-incompetent murine myeloid cells. Exp Hematol 1996; 24:214–20.

[2] Dong F, van Paassen M, van Buitenen C, Hoefsloot LH, Lowenberg B, Touw IP. A point mutation in the granulocyte colony-stimulating factor receptor (G-CSF-R) gene in a case of acute myeloid leukemia results in the overexpression of a novel G-CSF-R isoform. Blood 1995;85:902–11.

[3] Guba SC, Sartor CA, Hutchinson R, Boxer LA, Emerson SG. Granulocyte colony-stimulating factor (G-CSF) production and G-CSF receptor structure in patients with congenital neutropenia. Blood 1994;83:1486–92.

[4] Casadevall N, Nataf J, Viron B, Kolta A, Kiladjian JJ, Martin-Dupont P, et al. Pure red-cell aplasia and antierythropoietin antibodies in patients treated with recombinant erythropoietin. N Engl J Med 2002;346:469–75.

[5] Woiciechowsky C, Asadullah K, Nestler D, Eberhardt B, Platzer C, Schoning B, et al. Sympathetic activation triggers systemic interleukin-10 release in immunodepression induced by brain injury. Nat Med 1998;4:808–13.

[6] Takahashi S, Okamoto S, Shirafuji N, Oshima Y, Nagayama H, Shindo E, et al. Recombinant granulocyte-colony stimulating factor (rG-CSF)-combined conditioning with allogeneic bone marrow transplantation (BMT) for patients with acute myelogenous leukemia (AML). Blood 1995;86:358.

[7] Takahashi S, Oshima Y, Okamoto S, Nishiwaki K, Nagayama H, Inoue T, et al. Recombinant human granulocyte colony-stimulating factor (G-CSF) combined conditioning regimen for allogeneic bone marrow transplantation (BMT) in standard-risk myeloid leukemia. Am J Hematol 1998;57:303–8.

[8] Xie L, Zhang YL, Zhang ZY. Design and characterization of an improved protein tyrosine phosphatase substrate-trapping mutant. Biochemistry 2002;41:4032–9.

[9] Mishra AK, Zhang A, Niu T, Yang J, Liang X, Zhao ZJ, et al. Substrate specificity of protein tyrosine phosphatase: differential behavior of SHP-1 and SHP-2 towards signal regulation protein SIRPalpha1. J Cell Biochem 2002;84:840–6.

[10] Zhang ZY. Protein tyrosine phosphatases: structure and function, substrate specificity, and inhibitor development. Annu Rev Pharmacol Toxicol 2002;42:209–34.

[11] Savage DG, Antman KH. Imatinib mesylate—a new oral targeted therapy. N Engl J Med 2002;346:683–93.

[12] Oshima Y, Puri RK. A novel interleukin 13 (IL-13) antagonist that blocks the biological activity of human IL-13 in immune and nonimmune cells. FASEB J 2001;15:1469–71.

[13] Oshima Y, Puri RK. Characterization of a powerful high affinity antagonist that inhibits biological activities of human interleukin-13. J Biol Chem 2001;276:15185–91.

[14] Hage T, Sebald W, Reinemer P. Crystal structure of the interleukin-4/receptor alpha chain complex reveals a mosaic binding interface. Cell 1999;97:271–81.

[15] Aritomi M, Kunishima N, Okamoto T, Kuroki R, Ota Y, Morikawa K. Atomic structure of the GCSF-receptor complex showing a new cytokine-receptor recognition scheme. Nature 1999;401:713–7.
[16] Layton JE, Iaria J, Nicholson SE. Neutralising antibodies to the granulocyte colony-stimulating factor receptor recognise both the immunoglobulin-like domain and the cytokine receptor homologous domain. Growth Factors 1997;14:117–30.
[17] Altmann SW, Kastelein RA. Rational design of a mouse granulocyte macrophage-colony-stimulating factor receptor antagonist. J Biol Chem 1995;270:2233–40.
[18] Auguste P, Robledo O, Olivier C, Froger J, Praloran V, Pouplard-Barthelaix A, et al. Alanine substitution for Thr268 and Asp269 of soluble ciliary neurotrophic factor (CNTF) receptor alpha component defines a specific antagonist for the CNTF response. J Biol Chem 1996;271:26049–56.
[19] Chen WY, Wight DC, Wagner TE, Kopchick JJ. Expression of a mutated bovine growth hormone gene suppresses growth of transgenic mice. Proc Natl Acad Sci U S A 1990;87:5061–5.
[20] Chen W, Chen N, Yun J, Wagner T, Kopchick J. In vitro and in vivo studies of antagonistic effects of human growth hormone analogs. J Biol Chem 1994;269:15892–7.
[21] Harding PA, Wang X, Okada S, Chen WY, Wan W, Kopchick JJ. Growth hormone (GH) and a GH antagonist promote GH receptor dimerization and internalization. J Biol Chem 1996;271:6708–12.
[22] Hercus TR, Bagley CJ, Cambareri B, Dottore M, Woodcock JM, Vadas MA, et al. Specific human granulocyte-macrophage colony-stimulating factor antagonists. Proc Natl Acad Sci U S A 1994; 91:5838–42.
[23] de Hon FD, Dhlers M, Rose-John S, Ebeling SB, Bos HK, Aarden LA, et al. Development of an interleukin (IL) 6 receptor antagonist that inhibits IL-6-dependent growth of human myeloma cells. J Exp Med 1994;180:2395–400.
[24] Hudson KR, Vernallis AB, Heath JK. Characterization of the receptor binding sites of human leukemia inhibitory factor and creation of antagonists. J Biol Chem 1996;271:11971–8.
[25] Kim YS, Maslinski W, Zheng XX, Stevens AC, Li XC, Tesch GH, et al. Targeting the IL-15 receptor with an antagonist IL-15 mutant/Fcγ2a protein blocks delayed-type hypersensitivity. J Immunol 1998;160:5742–8.
[26] Kruse N, Tony HP, Sebald W. Conversion of human interleukin-4 into a high-affinity antagonist by a single amino-acid replacement. EMBO J 1992;11:3237–44.
[27] Kruse N, Shen B, Arnold S, Tony H, Meuller T, Sebald W. Two distinct functional sites of human interleukin 4 are identified by variants impaired in either receptor binding or receptor activation. EMBO J 1993;12:5121–9.
[28] Mellado M, Rodriguez-Frade JM, Kremer L, von Kobbe C, de Ana AM, Merida I, et al. Conformational changes required in the human growth hormone receptor for growth hormone signaling. J Biol Chem 1997;272:9189–96.
[29] Meropol NJ, Altmann SW, Shanafelt AB, Kastelein RA, Johnson GD, Prystowsky MB. Requirement of hydrophilic amino-terminal residues for granulocyte-macrophage colony-stimulating factor bioactivity and receptor binding. J Biol Chem 1992;267:14266–9.
[30] Pettit DK, Bonnert TP, Eisenman J, Srinivasan S, Paxton R, Beers C, et al. Structure–function studies of interleukin 15 using site-specific mutagenesis, polyethylene glycol conjugation, and homology modeling. J Biol Chem 1997;272:2312–8.
[31] Sundstrom M, Lundqvist T, Rodin J, Giebel LB, Milligan D, Norstedt G. Crystal structure of an antagonist mutant of human growth hormone, G120R, in complex with its receptor at 2.9 A resolution. J Biol Chem 1996;271:32197–203.
[32] Tavernier J, Tuypens T, Verhee A, Plaetinck G, Devos R, Vander Heyden J, et al. Identification of receptor-binding domains on human interleukin 5 and design of an interleukin 5-derived receptor antagonist. Proc Natl Acad Sci U S A 1995;92:5194–8.
[33] Tony H-P, Shen B-J, Reusch P, Sebald W. Design of human interleukin-4 antagonists inhibiting interleukin-4-dependent and interleukin-13-dependent responses in T-cells and B-cells with high efficiency. Eur J Biochem 1994;225:659–65.
[34] Vernallis AB, Hudson KR, Heath JK. An antagonist for the leukemia inhibitory factor receptor inhibits leukemia inhibitory factor, cardiotrophin-1, ciliary neurotrophic factor, and oncostatin M. J Biol Chem 1997;272:26947–52.
[35] Wang Y, Shen B-J, Sebald W. A mixed-charged pair in human interleukin. 4 dominates high-affinity interaction with the receptor alpha chain. Proc Natl Acad Sci U S A 1997;94:1657–62.
[36] Weigel U, Meyer M, Sebald W. Mutant proteins of human interleukin 2. Renaturation yield, proliferative activity and receptor binding. Eur J Biochem 1989;180:295–300.
[37] Kirito K, Nakajima K, Watanabe T, Uchida M, Tanaka M, Ozawa K, et al. Identification of the human erythropoietin receptor region required for Stat1 and Stat3 activation. Blood 2002;99:102–10.
[38] Oh-eda M, Hasegawa M, Hattori K, Kuboniwa H, Kojima T, Orita T, et al. O-linked sugar chain of human granulocyte colony-stimulating factor protects it against polymerization and denaturation allowing it to retain its biological activity. J Biol Chem 1990;265:11432–5.
[39] Cunningham BC, Ultsch M, de Vos AM, Mulkerrin MG, Clauser KR, Wells JA. Dimerization of the extracellular domain of the human growth hormone receptor by a single hormone molecule. Science 1991;254:821–5.
[40] de Vos AM, Ultsch M, Kossiakoff AA. Human growth hormone and extracellular domain of its receptor: crystal structure of the complex. Science 1992;255:306–12.
[41] Oshima Y, Joshi BH, Puri RK. Conversion of interleukin-13 into a high affinity agonist by a single amino acid substitution. J Biol Chem 2000;275:14375–80.
[42] Oshima Y, Tojo A, Niho Y, Asano S. Biological activity of human granulocyte colony stimulating factor with a modified C-terminus. Biochem Biophys Res Commun 2000;267:924–7.
[43] Brandhuber BJ, Boone T, Kenney WC, McKay DB. Three-dimensional structure of interleukin-2. Science 1987;238:1707–9.
[44] Brandhuber BJ, Boone T, Kenney WC, McKay DB. Crystals and a low resolution structure of interleukin-2. J Biol Chem 1987; 262:12306–8.
[45] Feng Y, Klein BK, McWherter CA. Three-dimensional solution structure and backbone dynamics of a variant of human interleukin-3. J Mol Biol 1996;259:524–41.
[46] Powers R, Garrett DS, March CJ, Frieden EA, Gronenborn AM, Clore GM. Three-dimensional solution structure of human interleukin-4 by multidimensional heteronuclear magnetic resonance spectroscopy. Science 1992;256:1673–7.
[47] Milburn MV, Hassell AM, Lambert MH, Jordan SR, Proudfoot AE, Graber P, et al. A novel dimer configuration revealed by the crystal structure at 2.4 A resolution of human interleukin-5. Nature 1993;363:172–6.
[48] Chow D, He X, Snow AL, Rose-John S, Garcia KC. Structure of an extracellular gp130 cytokine receptor signaling complex. Science 2001;291:2150–5.
[49] Somers W, Stahl M, Seehra JS. 1.9 A crystal structure of interleukin 6: implications for a novel mode of receptor dimerization and signaling. EMBO J 1997;16:989–97.
[50] Zdanov A, Schalk-Hihi C, Gustchina A, Tsang M, Weatherbee J, Wlodawer A. Crystal structure of interleukin-10 reveals the functional dimer with an unexpected topological similarity to interferon gamma. Structure 1995;3:591–601.
[51] Josephson K, Logsdon NJ, Walter MR. Crystal structure of the IL-10/IL-10R1 complex reveals a shared receptor binding site. Immunity 2001;15:35–46.
[52] Eisenmesser EZ, Horita DA, Altieri AS, Byrd RA. Solution structure of interleukin-13 and insights into receptor engagement. J Mol Biol 2001;310:231–41.